11-18-2016

Relaxation in bolted assemblies

Samuel Augustus Moeller
Rowan University

RELAXATION IN BOLTED ASSEMBLIES

by

Samuel Moeller

A Thesis

Submitted to the
Department of Civil and Environmental Engineering
College of Engineering
In partial fulfillment of the requirement
For the degree of
Master of Science in Civil Engineering
at
Rowan University
November 17, 2016

Thesis Chair: Douglas Cleary, Ph.D.

Dedication

I would like to dedicate this manuscript to my family, friends, and professors.

Acknowledgements

I would like to express my gratitude to Dr. Douglas Cleary and Dr. William Riddell for their flexibility and cooperation with me throughout my research. I would also like to thank my family and friends for encouraging me to finish this thesis. I would also like to thank those before me who provided the experimental data necessary to calibrate the simulation, without whom, this report would not have been possible to complete.

Abstract

Samuel Moeller
RELAXATION IN BOLTED ASSEMBLIES
2015-2016
Douglas Cleary, Ph. D.
Master of Science in Civil Engineering

The purposes of this investigation were to (a) extend previously developed elastic spring models for bolt assemblies to include simulating creep loss in the bolt and the threads and (b) to present an approach in which appropriate spring stiffness in the model are determined rationally. Previous efforts at modeling tension in bolts have been limited in that they were not readily applicable to analyses of realistic bolted connections. The simulated load distributions on the shank and the threads in a single-bolt assembly showed good comparison to the gathered experimental data as did the simulated, time dependent creep loss in the bolt. The ultimate goal of this research is to develop a model that includes nonlinear behavior that is suitable for investigating realistic multi-bolt connections.

Table of Contents

Abstract v

List of Figures viii

List of Tables ix

Chapter 1: Introduction 1

1.1 Background 1

1.2 Study Objectives 2

1.3 Thesis Organization 2

Chapter 2: Review of Literature 4

2.1 Early Studies 4

2.2 Elastic Spring Models 5

2.3 Experimental Studies of Bolt Tension Loss 6

2.4 Finite Element Studies 8

2.5 Research Significance 9

Chapter 3: Experimental Procedure 11

Chapter 4: Numerical Methodology 18

4.1 Numerical Model 18

4.2 Linear Elastic Behavior 18

4. 2. 1 Calibration of independent parameters 29

4.3 Non-Linear Behavior 32

4.4 Time-Dependent Behavior 36

4. 4. 1 Simulation of losses over time 51

Table of Contents (Continued)

4. 4. 2 Calibration of independent parameters 53

Chapter 5: Numerical Results and Discussion 56

5.1 Linear Elastic Model 56

5.2 Non-Linear Model 57

5.3 Time Dependent Model 62

Chapter 6: Conclusions & Recommendations 64

6.1 Summary of Findings 64

6. 1. 1 Linear elastic behavior 64

6. 1. 2 Non-linear behavior 66

6. 1. 3 Time dependent behavior 66

6.2 Conclusions 66

6.3 Recommendations 66

References 68

Appendix A: Proof – Show that $[C_{fd}]\,[C_{dd}]^{-1}[C_{df}] = [C_{ff}]$ 70

Appendix B: Proof – Show that $[C_{df}] + [C_{dd}][D] = 0$ 73

Appendix C: Simulation Code ..... .74

List of Figures

Figure Page

Figure 1. Configuration for Experiments 11

Figure 2. Bolt Rotation – 3/4 in. (a.) 1 (b.) 2 (c.) 4 & (d.) All Threads Remaining 14

Figure 3. Bolt Rotation – 7/8 in. (a.) 1 (b.) 2 (c.) 4 & (d.) All Threads Remaining 16

Figure 4. Schematic of Spring Model 21

Figure 5. Schematic Model for Single Thread Assembly 35

Figure 6. Schematic of Kelvin Model 36

Figure 7. Bolt-Nut Assembly Schematic for Time Dependent Behavior 40

Figure 8. Experimental Relaxation Data [9] 54

Figure 9. Experimental vs. Numerical Stiffnesses – 3/4 in. Bolt 57

Figure 10. Experimental vs. Numerical Stiffnesses – 7/8 in. Bolt 57

Figure 11. Non-Linear Behavior - 3/4 in. Bolt 58

Figure 12. Non-Linear Behavior – 7/8 in. Bolt 59

Figure 13. Thread Load Distribution – 3/4 in. Bolt 60

Figure 14. Thread Load Distribution – 7/8 in. Bolt 60

Figure 15. Thread Load Distribution Comparison 61

Figure 16. Experimental vs. Simulated Losses - 7/8 in. Bolt 62

List of Tables

Table Page

Table 1. Bolt Dimensions 12

Table 2. Test Matrix 13

Table 3. Average Results for Tests on 3/4 in. Bolts 15

Table 4. Average Results for Tests on 7/8 in. Bolts 17

Table 5. Node Numbering for Model. 20

Table 6. Linear Elastic Stiffness's Between Nodes. 22

Table 7. Node Numbering for Model 38

Table 8. Linear Elastic Constants Between Nodes 41

Table 9. Stiffnesses of ASTM A325 Bolts 65

Chapter 1

Introduction

1.1 Background

Bolted connections are one of the most common elements in structural design. They consist of threaded fasteners that join various components of a structural system. An axial load is applied to the fasteners by torqueing the bolt to an initial pretension. The rotation of the nut effectively shortens the distance between the nut and head, which leads to a tensile load in the bolt and a compressive load in the material being bolted. This load is transferred across the threads in the bolt/nut assembly causing displacement in the threads. Past studies investigating the distribution of forces in bolts and bolt threads have applied a load at the shank of the bolt to determine the resulting distribution on the threads. A modification of how the load is applied is important to this research and will be discussed.

After the initial pretension has been applied, the connection loses some of its tension [9]. Understanding the relaxation that occurs in bolted assemblies plays an important role in the future of connection design. At the moment, relaxation is not understood on the level needed to properly account for it in the design of connections. It is typically accounted for through the use of conservative design practices which lower the capacity of the connection. The capacity is lowered to a point conservatively below that of the actual force loss that can be expected from relaxation. While this has been effective, the continued study of this behavior is necessary to design more precise and more advanced connections.

1.2 Study Objectives

The objectives of this research are listed as follows:

- Review published research on load distribution and relaxation in bolted assemblies.
- Develop a rational method for calculating the load distribution on the threads of a bolted connection using linear elastic springs.
- Extend the linear method for determining the load distribution by incorporating thread yielding to capture behavior at higher bolt tension loads.
- Use experimental data to calibrate the nonlinear model.
- Develop a model that simulates relaxation load loss using linear elastic springs and viscous dashpots.
- Compare previous research to the objectives of the research in this paper identify differences, and propose directions for additional research.

1.3 Thesis Organization

This thesis is organized into six chapters. In Chapter 1, background information, the objectives of this study, and the organization of this report are presented. Chapter 2 consists of a comprehensive review of literature published on the topic. In Chapter 3 the experimental work that produced the data needed to calibrate the simulation is described. Chapter 4 describes the models for determining the load distribution in the bolt threads from an initial pretension assuming elastic behavior and non-linear behavior. In Chapter 4 the model that simulates relaxation in a bolted assembly is also discussed. In Chapter 5 comparisons between model and experimental results are made. Finally, Chapter 6

provides a summary of the research and the conclusions drawn. Recommendations for future studies are also made in this chapter.

Chapter 2

Review of Literature

2.1 Early Studies

The determination of the load distribution on threads is important in understanding the behavior of a bolted connection. For the better part of the last century there have been many studies dedicated to the load distribution on threads using a variety of experimental, analytical, and numerical approaches. Goodier [1] references the works of Jaquet and Den Hartog, who presented solutions to the location of the load concentration on a connection and how that would affect an evenly distributed load on the threads. Jaquet and Den Hartog observed a large concentration of load at the base of the nut which causes the threads to yield at lower loads than the bolt, modifying the distribution [1]. The first method for determining the distribution of load along the threads of a bolt was to observe axial and radial thread displacements as the connection was loaded with a mirror extensometer on the outside of a nut. The thread displacements were then used to determine the average axial stress over the wall thickness of the nut at any cross-section. Once the average axial stress is known, the load distribution can be found [1]. Bolts that carried only a single turn of thread at the free end, middle, and base of the nut were used to produce an artificial concentration of load which showed that there is not a uniform distribution [1].

Hetenyi [2] used a photoelastic "stress freezing" method to determine the stress distribution in bolted connections. This process involved the use of connections made of Bakelite^{TM} due to its photoelastic properties. Under loaded conditions the model was

annealed to very high temperatures and cooled back to room temperature. This "froze" the elastic stresses and deformations experienced upon loading, and, by taking a photoelastic picture of the bolt model, a qualitative distribution of stresses could be produced [2]. Results showed that the stress concentration was highest at the end of the nut closest to the clamped surface, and that most of the load is transmitted between the first engaged thread and the nut. These conclusions compared well with those of Hetenyi's predecessors.

Sopwith [3] was the first to present theoretical work that included radial expansion which he ultimately compared with the experimental studies of [1]. Using an analytical solid mechanics approach, the distribution of load along threads throughout the bolt assembly was determined [3]. Sopwith's analytical results agreed well with the previously published experimental results [1, 2]. Various degrees of thread yielding were considered and the effect of these variations on the distribution of load along the nut was discussed. Sopwith graphically describes the load distribution on the threads for the various extents of yielding. This theoretical method included both a compression and tension case and concluded that the distribution of load to the threads was not uniform due to strains in the bolt and nut under load, but as yielding progresses, the load distribution along the threads becomes more uniform [3].

2.2 Elastic Spring Models

Miller *et al*. [4], Curti and Raffa [5], and Wang and Marshek [6] have all developed elastic spring models to model bolt-nut assemblies. Miller *et al*. [4] and Curti and Raffa [5] developed models for both the tension (turnbuckle) and compression (nut and bolt) cases. Miller *et al*. [4] described the load distribution using second order finite

difference equations and verified the mathematics by comparing the solution to a finite element analysis and the experimental results of Sopwith [3] and Hetenyi [2]. Curti and Raffa [5] used a linear elastic one dimensional model of a joint to investigate the load distribution on threads of a bolted connection. These authors concluded that a linear elastic spring model is an effective way to model the load distribution across the threads of a bolt. Wang and Marshek [6] extended the spring model presented by Miller, *et al*. [4] to allow for the yielding of individual threads. For this model, the yield strength of each thread was determined from a mechanics-based model for the deformation of the threads and a Tresca model for yield. Additional spring-based models have been developed where the stiffness of various components of an assembly are combined. For example, Fukuoka and Takaki [7] considered separate stiffness values for the springs representing clamping interfaces, engaged threads, exposed threads, bolt body, bolt head, and fastened plate.

2.3 Experimental Studies of Bolt Tension Loss

Chesson and Munse [8] perform experimental studies on bolted assemblies which significantly differ from all the previous authors. The majority of their study focuses on whether washers can be eliminated from a high-strength bolted assembly without sacrificing the integrity of the connection. However, within this study they perform a series of relaxation tests on A325 bolts to determine how much tension is lost in a bolted connection over time. Strain readings were taken periodically after tightening and these tests lasted 5 minutes or from 3 to 90 days. It was found that one minutes after tensioning the load dropped between 2-11 percent with an average of 5 percent. The assemblies undergoing longer term tests saw an additional 5% losses relative the load remaining

after 1 minute and the 90% of the total losses still occurred within the first day. These losses they believe can be attributed to elastic recovery or potentially creep and yielding.

Reuther, D. et al. [9] further addresses the time dependent aspect to the load in a threaded connection. Various tensioning methods, bolt diameters, and lengths were used in the experimental procedure and the objective was to determine what variables have the largest effect on the relaxation in a bolted assembly. The experimental results conclude that the hardware of a bolted connection has little to no influence on the relaxation of the bolt. The relaxation observed in the bolt over time can be attributed to the diameter and the initial pre-tensioning of the bolt with a linear relationship found between the pretension force and percent losses.

Yang and DeWolf [10] performed studies which addressed losses in galvanized coated structural connections. The objective was to come up with a mathematical model which would predict the relaxation of the clamping force. It was observed that losses were greater when the galvanized coating was thicker due to a decrease in slip resistance between the bolt and the clamped surface. The losses ranged between 10-20% for various coating thicknesses and it was found that 90% of the losses occurred in the first week of the test. The experimental data was then used to develop the analytical model which depicts the bolt as a single spring. The reduction in the tensile force is attributed to elastic losses after tightening and creep losses in the galvanized coating layer and steel relaxation in the bolt.

As a result of stricter standards in building codes for overall energy consumption in buildings, Oostdyk [11] conducted research on the losses that occur at the transfer of loads in connections with thermal barriers. Connection configurations consisted of

typical, bolted steel-to-steel plates, steel plates bolted with a thermal break plate sandwiched in the middle, and a similar configuration with a thermal plate and thermal washers. It was concluded that the thermal break plate connection with regular washers saw lower losses than the typical all steel connections while the utilization of the thermal washers increased the losses significantly. Larger diameter washers did, however, decrease the overall observed losses.

2.4 Finite Element Studies

Maruyama [12] used the finite element method in conjunction with the point-matching method to determine the stress concentration of a threaded connection. In the computations for the FEM a modulus of elasticity of E = 21,000 kg/mm2 is used with Poisson's ratio as $\nu = 0.3$. These material properties are common in standard spring steel. Grades SCM 3 and S45C steel were used to fabricate the bolt and nut for the copper-electroplating method, respectively. The value for the stress concentration factor obtained from the finite element method agreed well with that obtained experimentally through the copper-electroplating method. However, he concludes that due to many stress concentration points and, for the reason of element divisions, it is difficult to model a structure with a complicated form such as a screw thread using the finite element method.

Tanaka [13] develops a fundamental method for the finite element analysis of bolt-nut connections. His goal is to create a more practical method than Maruyama's FEM – point matching method. He compares his two-dimensional FEM to a simple one-dimensional spring model because the implementation of the point-matching method on a structure with many contact surfaces, such as a threaded connection, is inefficient. He used a modulus of elasticity of E=21,200 kgf/mm2 with a Poisson's ratio of $\nu = 0.3$ in his

bolt-nut models. As was the case with Maruyama's bolt-nut assembly, these properties are common in spring steel. The load distribution obtained from the spring model agreed relatively well with that obtained from the finite element analysis of the connection.

Varadi and Joanovics [14] developed a non-linear finite element model with contact elements to evaluate the contact state of a bolt-nut-washer-compressed shear joint system. The non-linear axisymmetric model with contact elements is suitable to analyze the bolted joint having parts with different strength properties, to find the plastic zones, to obtain the load distributions among threads in contact, to determine the real preload diagram of the bolted joint system.

2.5 Research Significance

Extending the previously developed elastic spring models for bolt assemblies to include load loss from relaxation in the bolt and the threads, while presenting a rational approach to determine appropriate spring and dashpot stiffnesses is part of what distinguishes this study from past research. The ultimate goal is to lay the groundwork for a model that includes nonlinear time-dependent behavior that is suitable for investigating realistic multi-bolt connections. Previous efforts at modeling tension in bolts have been limited in that they were not readily applicable to analyses of realistic bolted connections. On one hand, analytical and finite element analyses that have incorporated nonlinearity due to material behavior and contact are likely too complex to incorporate into models of realistic bolted connections that can be used for a sensitivity study for developing design procedures. On the other hand, spring models that use an FEA-based formulation, while simple enough to incorporate into a model of a realistic connection, do not incorporate nonlinear behavior observed at bolt tensions approaching

the strength of the bolt. Spring-based models also do not incorporate time dependent behaviors observed at typical values of pretensioning, both of which are usually seen in practice in structural assemblies. In this work, data from experiments on single thread bolt-nut assemblies is used to calibrate full thread, linear and nonlinear spring-based models, which predict the load distribution for assemblies with various clamp lengths. The simulation results of the full thread model agree with experimental observations for both 3/4 in. and 7/8 in. bolts. In both cases, the model predicts that threads are yielding at loads lower than the minimum pretension specified by the AISC code [16], justifying the need to capture nonlinear behavior. The linear spring model is then extended to capture time-dependent losses of bolt tension. The model presented in this thesis will allow researchers to move forward toward the modeling of the relaxation of bolted connections using nonlinear, time dependent conditions.

Chapter 3

Experimental Procedure

Tests were conducted on ASTM A325 7/8 in. and 3/4 in. steel bolts that were 3.5 in. long to record the force the bolt experiences due to an applied rotation and at what force the threads will yield. Figure 1 is an illustration of the test setup with key components and dimensions labeled. Table 1 summarizes the key parameters for both the 7/8 in. and 3/4 in. diameter bolt configurations. The nominal area of the threaded portion of a Unified National Coarse (UNC) bolt, A_t, is given by [16] and expressed with customary units in Equation 1.

$$A_t = 0.785(d - 0.9743p)^2 \quad (1)$$

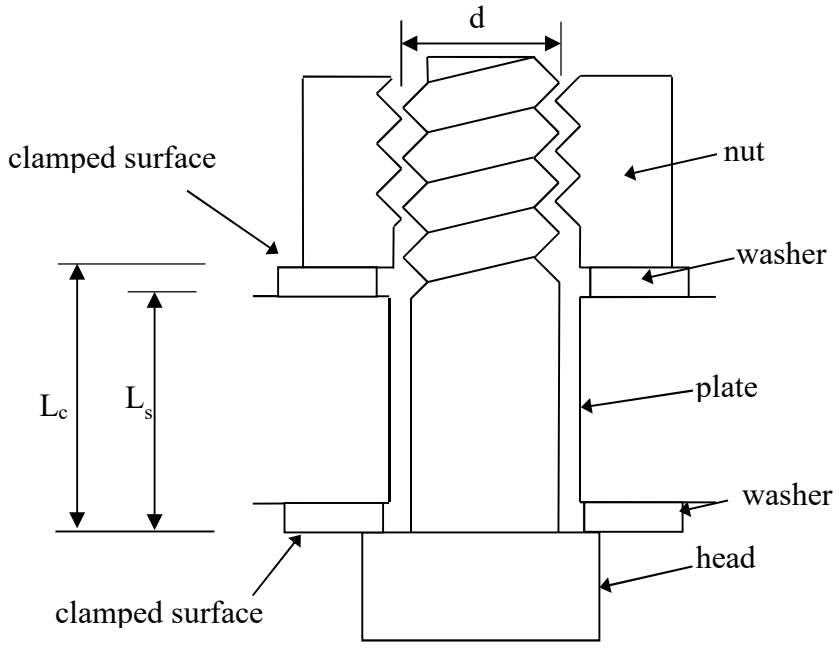

Figure 1. Configuration for Experiments

Table 1

Bolt Dimensions

Parameter	Description	3/4 in. diameter	7/8 in. diameter
L	Bolt Length, in	3.5	3.5
L_c	Clamp Length, in	2.035	1.948
L_s	Unthreaded length of the bolt, in	1.998	1.880
d	Diameter of the bolt, in	0.75	0.825
p	Pitch of the threads, in	0.10	0.11
A	Area of unthreaded portion of bolt, in^2	0.4418	0.6013
A_t	Nominal area of threaded portion of bolt, in^2	0.3343	0.4628

Bolts were placed in a bolt tension calibrator with a washer on either face of the load plate. Once in the bolt tension calibrator, the bolt was pre-tensioned to 5 kips. A mark was then made on the bolt tension calibrator to indicate the orientation of a marked edge of the nut (used as a zero mark). The bolts were tensioned until the twist-tension relation showed noticeable nonlinear behavior or failure, stopping to make marks on the bolt tension calibrator once certain predetermined tensions were reached. Once the testing was completed, the angle of rotation was measured using the marks made on the bolt tension calibrator. Because a 5 kip load was taken as the starting point, and therefore the 0 angle, the graphs made from the raw angle data were shifted to make 0 kips the 0 angle. This was done by finding the slope (m) and y-intercept (b) of the linear portion of the graph. Then (b/m) was added to every x-value on the graph making the x- and y-intercepts of the linear portion of the graph coincide with the origin. This approach is thought to avoid initial nonlinearities in the twist-tension relationship, which are felt to be inconsistent and can lead to an inaccurate set of data.

For some tests, threads were removed from the nuts before they were put on the bolt. These tests allowed calibration of the spring model parameters. The resulting test matrix is shown in Table 2. The 7/8 in. diameter unmodified nut has 7 complete rings of threads and the 3/4 in. unmodified nut has 6 complete rings of threads. Because the nuts with fewer threads remaining failed at lower tensioning force than nuts with more threads remaining, the angle measurements were taken at smaller tensioning intervals, e.g., the nuts with 1 thread remaining failed near 15 kips, so measurements were taken at every 1 kip interval; while the nuts with all threads remaining yielded near 50 kip, so measurements were taken at 5 kip intervals. This ensured that there were sufficient data to observe trends for each test.

Table 2

Test Matrix

Number of Tests	Number of Threads Remaining 3/4 in.	Number of Threads Remaining 7/8 in.
4	1	1
4	2	2
4	4	4
4	6 (All)	7 (All)

The angle measurements were obtained directly during the tests, as well as from photographs taken during the tests which were then analyzed using a commercial software package with an angle measurement feature. The two measurements were averaged to reduced variability. However, the difference between the physical and virtual measurements was less than 0.122 radians (7 degrees) in all cases.

Figure 2 illustrates the relationship between force and rotation for 3/4 in. bolts with (a) one thread remaining (b) 2 threads remaining (c) 4 threads remaining (d) all threads remaining. A straight line was fitted to the linear region of each curve to find the linear elastic stiffness.

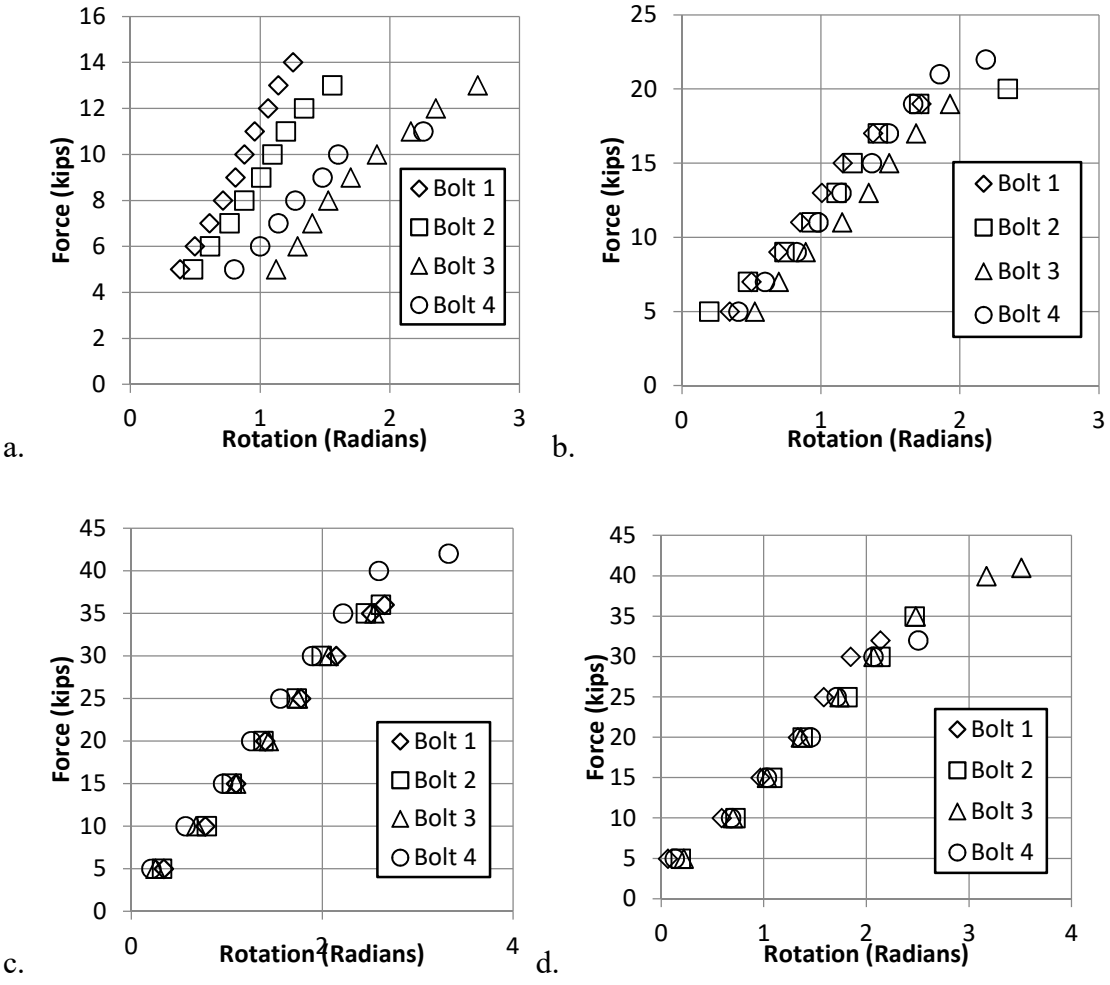

Figure 2. Bolt Rotation – 3/4 in. (a.) 1 (b.) 2 (c.) 4 & (d.) All Threads Remaining

The averages of the linear stiffness, m, and ultimate force, F_u, of the 3/4 in. nuts with 1 thread remaining, 2 threads remaining, 4 threads remaining, and all of the threads remaining are displayed in Table 3. The force was increased in 5 kip intervals for the

nuts with all threads remaining and 4 threads remaining, 2 kip intervals for nuts with 2 threads remaining, and 1 kip intervals for nuts with 1 thread remaining. The ultimate force is the maximum recorded force applied to the bolt in the last increment prior to failure of the bolt.

Table 3

Average Results for Tests on 3/4 in. Bolts

Number of Threads Remaining	m, lbs/radian	F_u, lbs
1	7963.775	12750
2	11468.9	20250
4	14610.75	38000
6	14678.5	37750

Figure 3 illustrates the relationship between force and rotation for 7/8 in. bolts with (a) one thread remaining (b) 2 threads remaining (c) 4 threads remaining (d) all threads remaining. A straight line was fitted to the linear region of each curve to find the linear elastic stiffness.

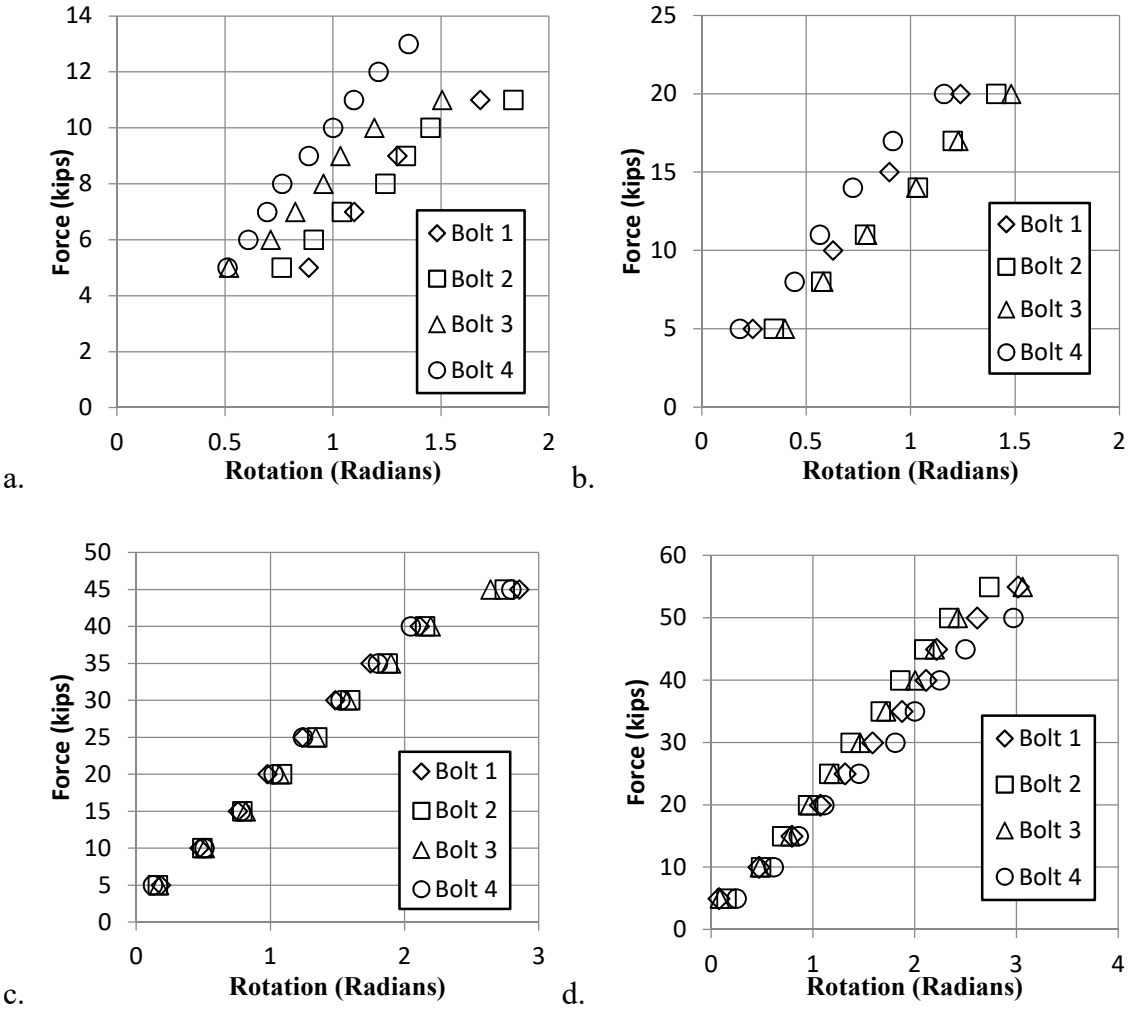

Figure 3. Bolt Rotation – 7/8 in. (a.) 1 (b.) 2 (c.) 4 & (d.) All Threads Remaining

The averages of the stiffness, m, and ultimate force, F_u, of the 7/8 in. nuts with 1 thread remaining, 2 threads remaining, 4 threads remaining, and all of the threads remaining are displayed in Table 4. The force was increased in 5 kip intervals for the nuts with all threads remaining and 4 threads remaining, 3 kip intervals for nuts with 2 threads remaining, and 1 kip intervals for nuts with 1 thread remaining. The ultimate

force is the maximum recorded force applied to the bolt in the last increment prior to failure of the bolt.

Table 4

Average Results for Tests on 7/8 in. Bolts

Number of Threads Remaining	m, lbs/radian	F_u, lbs
1	7966.075	11500
2	15738.75	23000
4	19295.5	45000
7	19529.5	57500

Chapter 4

Numerical Methodology

4.1 Numerical Model

Following the configuration of springs used by Tanaka *et al*. [13], Miller *et al*. [4], Curti and Raffa [5], Wang and Marshek [6], and Fukuoka and Takaki [7], a model is developed that is based on a simple configuration of springs representing the stiffness of the threads, bolt shank and the regions between the threads in both the nut and bolt. A FEA-based formulation similar to that used by Tanaka, *et al*. [13] is used to develop appropriate finite element global stiffness matrices. Following Wang and Marshek [6] and Fukuoka and Takaki [7] nonlinear behavior of the assembly is captured by allowing yielding of springs that represent each thread. The result is a model that extends those of Tanaka et al. [13], Miller et al. [4], and Curti and Raffa [5] with the addition of capturing the flexibility of the bolt shank and the nonlinear aspects of thread deformation.

First, the linear elastic aspect of the model is discussed, then the nonlinear behavior. Finally, time dependent behavior is addressed.

4.2 Linear Elastic Behavior

The linear elastic model is based upon a series of springs connected to nodes and solved as a matrix structural analysis problem, which can be thought of as a specialized finite element formulation. The configuration of the model is shown in Figure 4, and is similar to the configurations used by Tanaka et al. [13], Miller et al. [4], and Curti and Raffa [5]. The configuration shown represents an assembly with three threads engaged, but the model is general for arbitrary integer, n, of threads engaged. There is a node at

each clamped surface. There are 2 nodes corresponding to each thread: one on the bolt and one on the nut.

Each thread can be thought of as a small cantilever which deflects like any other member under loaded conditions. As such, the deflection is determined by Hooke's Law, represented in Equation 2.

$$F = kx \tag{2}$$

Where, x is the deflection, F is the applied force, and k is the thread stiffness, a property specific to the type of nut and bolt, and related to both material properties and geometric configuration.

In this model, displacements are constrained to occur only in the direction of the axis of the bolt. For a model with n threads, there are 2n+2 degrees of freedom. Of these, 2 are specified displacements (s), and 2n are free displacements (f). The numbering of these nodes is summarized in Table 5. The connectivity between nodes is as shown in Figure 4, with the stiffness between nodes denoted by k_1 through k_4. The parameter α determines where on the thread the load transfer occurs for the thread closest to the clamped surface. It is the reciprocal of the fraction of the pitch between load transfer and the clamped plate. These stiffnesses are summarized in Table 6. For these tables, threads are numbered such that 1 is furthest from the clamped surface, and n is closest to the clamped surface.

Table 5

Node Numbering for Model

Nodes	Description
1, 3, …, 2i-1, …, 2n-1	Center line of bolt at i^{th} thread.
2, 4, …, 2i, …, 2n	On the nut, corresponding to i^{th} thread.
2n+1	Center line of the bolt at the head.
2n+2	Boundary between nut and clamped plate.

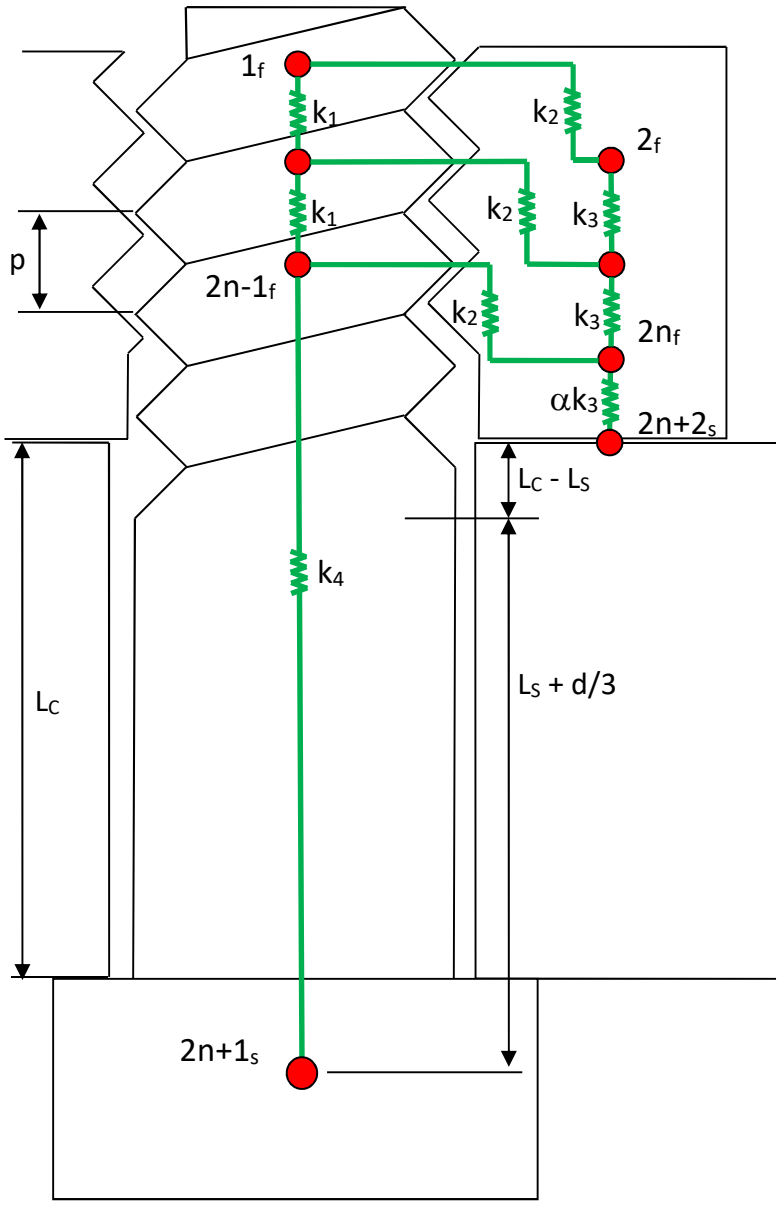

Figure 4. Schematic of Spring Model

The total force in the bolt is determined by calculating the stiffness in the shank multiplied by the change in distance between nodes 2n-1 and 2n+1 which, theoretically has an equal and opposite value to the sum of the load distributions on the threads. The stiffness of the shank is determined as a function of its length. This approach to calculating the shank stiffness differs from previous studies, where the shank length was not considered. Another key difference between this model and earlier approaches is how the load is applied to the bolt. Instead of applying a force at the first node of the threads a rotation is applied to the bolt head causing an initial pretension on the shank which is then transferred throughout the bolt.

Table 6

Linear Elastic Stiffness's Between Nodes

Stiffness	Connected Nodes	Description
k_1	2i-1 and 2i-3	Stiffness of bolt between thread i and i-1.
k_2	2i and 2i-1	Stiffness of thread i.
k_3	2i and 2i-2	Stiffness of nut between thread i and i-1.
αk_3	2n and 2n+2	Stiffness of nut between n^{th} thread and clamped plate.
k_4	2n-1 and 2n+1	Stiffness of bolt along effective clamped length.

The values for k_1 and k_4 are assumed to be predicted from a straightforward solid mechanics approach, and are therefore known *a priori*. The stiffness of the bolt between successive threads is given by

$$k_1 = \frac{A_t E}{p} \tag{3}$$

where A_t is the effective cross sectional area of the threaded portion of the bolt, E is the elastic modulus of the bolt, and p is the thread pitch. The stiffness of the bolt along the clamped length is given by

$$k_4 = \frac{1}{\frac{1}{\alpha k_1} + \frac{L_s + {}^{d}/_{3}}{AE} + \frac{L_c - L_s}{A_t E}} \tag{4}$$

where *A* is the area of the unthreaded portion of the bolt, L_s is the length of the unthreaded portion of the bolt and L_c is the clamp length. The dimension d/3 is added to the length of the shank, L_s, to approximate the effects of deformation of the bolt head. This quantity lies somewhere between the overall length of the bolt and the grip length. It is usually estimated as the grip length plus one half the thickness of the head and one half the thickness of the nut [15]. The αk_1 term captures the axial length required to effectively engage the first thread. The other two element stiffness's, k_2 and k_3, correspond to the stiffness of a single row of threads and the corresponding stiffness's of the nut along the length of one row of threads respectively. These values are not determined from a simple solid mechanics approach. Instead, they are determined from the experimental results presented in Chapter 3. The process for determining these values is described in the following sections.

The resulting equation for equilibrium is written in partitioned form in equation 5. The appropriate submatrices, $[K_{ff}]$, $[K_{fs}]$ and $[K_{ss}]$ are given in equations 6, 7, and 8 respectively. Note that the submatrix $[K_{sf}]$ can be determined from $[K_{fs}]$ from symmetry.

Note that node numbering is such that the global stiffness matrix is readily partitioned into K_{ff}, K_{fs}, K_{sf}, and K_{ss}. The resulting relationship for load and displacements is given by Equation 5.

$$\begin{Bmatrix} F_f \\ F_s \end{Bmatrix} = \begin{bmatrix} K_{ff} & K_{fs} \\ K_{sf} & K_{ss} \end{bmatrix} \begin{Bmatrix} U_f \\ U_s \end{Bmatrix} \tag{5}$$

Equation 6 shows submatrix K_{ff} .

$$K_{ff} = \begin{array}{c|cccccccc} & 1 & 2 & 3 & 4 & \cdots & 2n-2 & 2n-1 & 2n \\ \hline 1 & k_1+k_2 & -k_2 & -k_1 & & & & & \\ 2 & -k_2 & k_2+k_3 & 0 & -k_3 & & 0 & & \\ 3 & -k_1 & 0 & 2k_1+k_2 & -k_2 & -k_1 & & & \\ 4 & & -k_3 & -k_2 & k_2+2k_3 & 0 & \ddots & & \\ \vdots & & & -k_1 & 0 & \ddots & \ddots & -k_1 & \\ 2n-2 & & 0 & & \ddots & \ddots & k_2+2k_3 & 0 & -k_3 \\ 2n-1 & & & & & -k_1 & 0 & k_1+k_2+k_4 & -k_2 \\ 2n & & & & & & -k_3 & -k_2 & k_2+(1+\alpha)k_3 \end{array}$$

(6)

Equation 7 shows submatrix K_{fs} . Note that $K_{sf} = K_{fs}^{T}$.

$$K_{fs} = \begin{array}{c|cc} & 2n+1 & 2n+2 \\ \hline 1 & & \\ 2 & & \\ 3 & & \\ 4 & 0 & \\ \vdots & & \\ 2n-2 & & \\ 2n-1 & -k_4 & \\ 2n & 0 & -\alpha k_3 \end{array}$$

(7)

Equation 8 shows submatrix K_{ss} .

$$K_{ss} = \begin{array}{c|cc} & 2n+1 & 2n+2 \\ \hline 2n+1 & k_4 & 0 \\ 2n+2 & 0 & \alpha k_3 \end{array} \tag{8}$$

In practice, tension is applied to a bolt by turning the nut. The resulting movement of the nut along the axis of the bolt reduces the pre-strained length of the bolt that spans the grip length. Rather than shortening the grip length, tightening is simulated by displacing the node at the head of the bolt by a distance

$$u_{2n+1} = \frac{-p\theta}{2\pi} \tag{9}$$

where, p is the pitch of the thread and θ is the rotation of the nut from the zero-force rotation, measured in radians. Note that the model assumes linear behavior starting immediately from some baseline zero rotation. This is not the actual behavior observed in practice, rather a linear region is observed after a small, initial rotation causing slight nonlinearity [6]. The second displacement-specified node, 2n+2, is assumed to have zero displacement, resulting in a specified displacement vector which can be written as

$$\{U_s\} = \begin{Bmatrix} u_{2n+1} \\ u_{2n+2} \end{Bmatrix} = \begin{Bmatrix} \frac{-p\theta}{2\pi} \\ 0 \end{Bmatrix} \tag{10}$$

As there are no external forces applied, *i. e.* , $\{F_f\} = 0$, Equation 5 may be re-written to solve for the vector of free displacements

$$\{U_f\} = [K_{ff}]^{-1}(-[K_{fs}]\{U_s\}) \tag{11}$$

Once the free displacements are solved for, the load transferred by the i^{th} thread (numbered with 1 as the furthest from the clamped surface and n as the closest to the clamped surface), F_i, is given by

$$F_i = k_2(u_{2i} - u_{2i-1}) \tag{12}$$

The force in the bolt is given by

$$F_{n+1} = k_4(u_{2n-1} - u_{2n+1}) \tag{13}$$

4. 2. 1 Calibration of independent parameters. The model has four independent parameters k2, k3, α, and β. The results are relatively insensitive to α, which has been taken to be 1.0 for the analyses discussed in this thesis. The values for the linear elastic spring constants k2 and k3 may be established by considering the experimentally observed behavior of a bolt with a single thread. This case is considered in the schematic of Figure 6 that has only the degrees of freedom 2n-1 =1, 2n+1=3, and 2n+2=4. Note that the second degree of freedom has been removed, and the resulting stiffness is the equivalent stiffness of the two adjacent springs in series. Using the same spring stiffness coefficients as previously determined, we can relate the experimentally observed force in the bolt to

$$F_{bolt} = k_4(u_1 - u_3) = k_4 U_b \tag{14}$$

Where U_b represents the elongation of the shank of the bolt up to the beginning of the thread. Node 4 is fixed and therefore the displacement of node 1 is simply the change in position caused by combined thread and nut deformation, denoted U_{t+n}.

$$U_{t+n} = u_1 \tag{15}$$

Because k_4 is in parallel with k_2 and αk_3, which are in series, the force in the bolt can be redefined based on the equilibrium of the model.

$$-F_{bolt} = \frac{1}{\frac{1}{k_2} + \frac{1}{\alpha k_3}} U_{t+n} \tag{16}$$

From Equation 10, the displacement of node 3 is related to the rotation of the nut by

$$u_3 = u_{2n+1} = \frac{-p\theta}{2\pi} \tag{17}$$

Now that the variables in Equation 14 have been defined based on the model, they can be entered into the equation which can then be rearranged so that k_2 and αk_3 are defined explicitly. First, Equations 15 and 17 are substituted into Equation 14, resulting in

$$F_{bolt} = k_4 u_{t+n} + k_4 \frac{p\theta}{2\pi} \tag{18}$$

Substituting Equation 16 into Equation 18 results in

$$-\frac{1}{\frac{1}{k_2} + \frac{1}{\alpha k_3}} U_{t+n} = k_4 U_{t+n} + k_4 \frac{p\theta}{2\pi} \tag{19}$$

Rearranging Equation 19 results in

$$-\frac{1}{k_4} = \frac{\left(\frac{p\theta}{2\pi}\right)\left(\frac{1}{k_2} + \frac{1}{\alpha k_3}\right)}{U_{t+n}} + \left(\frac{1}{k_2} + \frac{1}{\alpha k_3}\right) \tag{20}$$

Substituting Equation 16 back into Equation 20 and rearranging, the result gives

$$\frac{p\theta}{2\pi F_{bolt}} - \frac{1}{k_4} = \left(\frac{1}{k_2} + \frac{1}{\alpha k_3}\right) \tag{21}$$

or in terms of the force-twist relationship

$$\frac{p}{2\pi}\frac{d\theta}{dF_{bolt}} - \frac{1}{k_4} = \left(\frac{1}{k_2} + \frac{1}{\alpha k_3}\right) \tag{22}$$

where $\frac{d\theta}{dF_{bolt}}$ is the torque-twist flexibility in a bolt assembly with one thread, as determined by laboratory experiments, so that only the right hand side of the equation has unknown values. Finally, the right hand side of Equation 22 can be split so that the individual k_2 and αk_3 values can be found. This results in the development of a parameter, β, which is arbitrary at this point.

$$\frac{1}{k_2} = \beta\left(\frac{p}{2\pi}\frac{d\theta}{dF_{bolt}} - \frac{1}{k_4}\right) \tag{23}$$

and

$$\frac{1}{\alpha k_3} = (1-\beta)\left(\frac{p}{2\pi}\frac{d\theta}{dF_{bolt}} - \frac{1}{k_4}\right) \tag{24}$$

For any given pair of α and β the model predicts a load distribution on the threads of the bolt-nut assembly and the force in the bolt along the clamped length. In the case where the rotation of the nut, θ, is equal to 1 radian, the predicted force in the bolt is equivalent to the stiffness of the bolted assembly. Units for stiffness of the bolted assembly are kips per radians. For the case of a bolt with a single thread, this numerical stiffness value equals the experimentally determined value regardless of the value of β. However, the value of β will affect predictions for bolts with additional threads. Therefore, experimentally observed stiffnesses for fully threaded assemblies can be used to determine the appropriate value of β. This was accomplished by performing multiple iterations where β started at the arbitrarily chosen value of 0.85 and stepped through at intervals of 0.001 until the resulting numerical stiffness was equal to the experimental value for bolted assemblies with full threads intact to a ±0.002 kip/radian tolerance. Through this process, it was found that for a 3/4 in. diameter A325 bolt, β was equal to 0. 872, and for a 7/8 in. diameter A325 bolt, β was equal to 0.933. The k_2 and k_3 values for a 3/4 in. diameter bolt were 634.4 kips/radians and 2161 kips/radians respectively. The k_2 and k_3 values for a 7/8 in. diameter bolt were 523.9 kips/radians and 3768 kips/radians respectively.

4.3 Non-Linear Behavior

Non-Linear analyses are carried out using an incremental approach. The matrix equation that corresponds to the differential of Equation 5 is

$$\begin{Bmatrix} dF_f \\ dF_s \end{Bmatrix} = \begin{bmatrix} K_{ff_t} & K_{fs_t} \\ K_{sf_t} & K_{ss_t} \end{bmatrix} \begin{Bmatrix} dU_f \\ dU_s \end{Bmatrix} \tag{25}$$

Where the subscript t on the submatrices identifies them as tangential stiffnesses. The stiffness matrices originate as the linear elastic stiffness matrices. Incremental values of $\{dU_s\}$ are applied, and resulting incremental values of $\{dU_f\}$ are calculated. After each step, member forces in the spring are evaluated. If a spring representing a thread is found to have surpassed yield load, only the fraction of the load increment prior to yielding is applied. Then, the tangential stiffness matrix is assessed a penalty corresponding to 95% of the linear elastic stiffness of the spring. New load increments are then applied until the next thread yields.

The incremental displacement vector $\{dU_s\}$ can be written in terms of an incremental twist of the nut, $d\theta$, as

$$\{dU_s\} = \begin{Bmatrix} du_{2n+1} \\ du_{2n+2} \end{Bmatrix} = \begin{Bmatrix} \frac{-pd\theta}{2\pi} \\ 0 \end{Bmatrix} \tag{26}$$

As there are no external forces applied, i.e., $\{F_f\}=0$, Equation 25 may be re-written to solve for the vector of incremental free displacements

$$\{dU_f\} = \left[K_{ff_t}\right]^{-1}\left(-\left[K_{fs_t}\right]\{dU_s\}\right) \tag{27}$$

Once the free displacements are solved for, the load transferred by the i^{th} thread (numbered with 1 as the furthest from the clamped surface and n as the closest to the clamped surface), F_i, is given by

$$F_i = F_{i_0} + dF_i = F_{i_0} + k_4(du_{2i} - du_{2i-1}) \quad (28)$$

The force in the bolt is given by

$$F_{n+1} = F_{n+1_0} + dF_{n+1} = F_{n+1_0} + k_4(du_{2n+1} - du_{2n-1}) \quad (29)$$

At the end of each step, the loads on individual threads are compared to the specified yield loads. If one or more threads are found to have yielded, the incremental $d\theta$ is reduced such that the load increment results in a single thread exactly reaching yield strength. The tangential stiffness is then changed using a penalty approach, and additional increments are then applied with the new tangential stiffness matrix until the next thread yields.

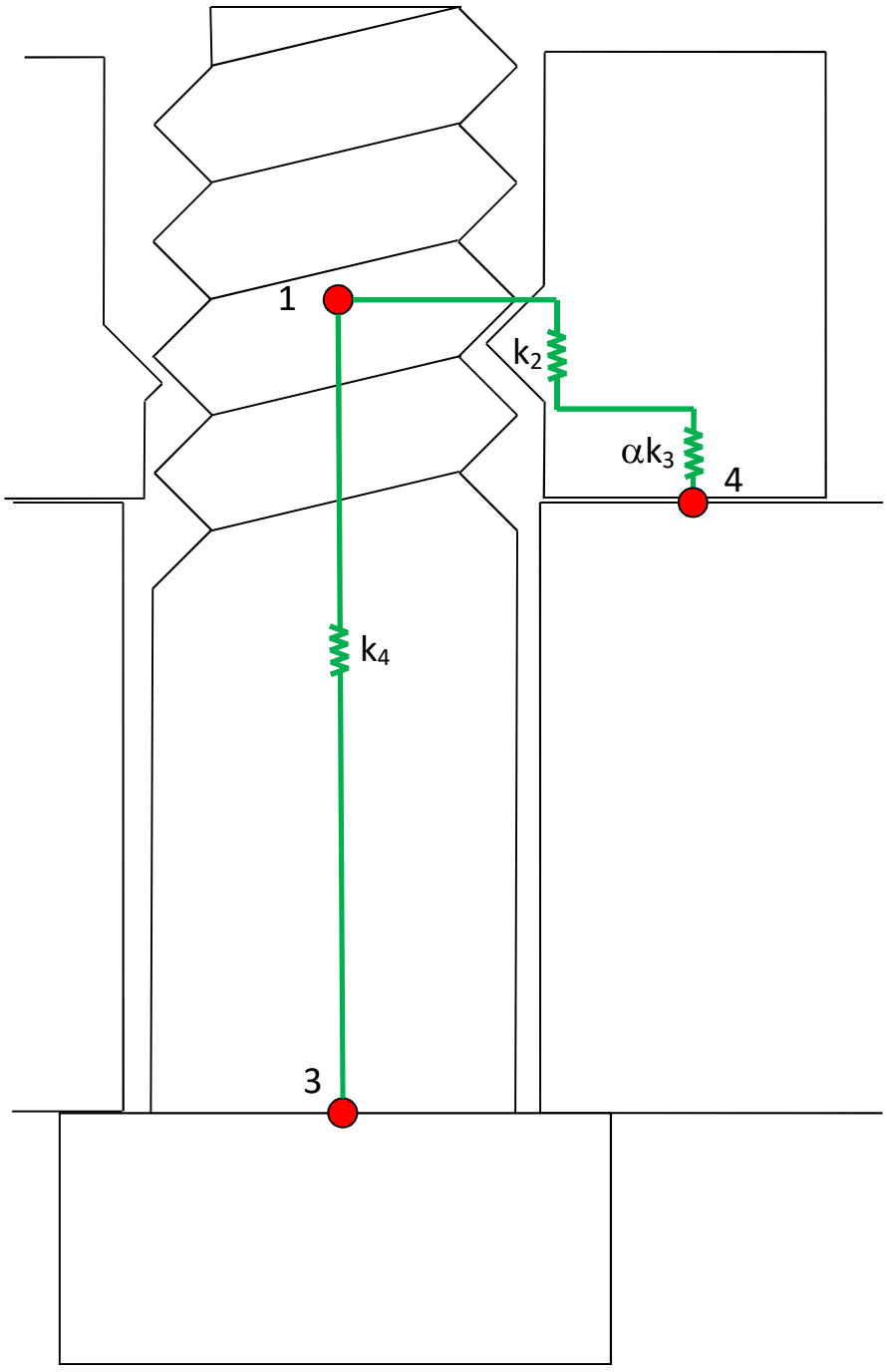

Figure 5. Schematic Model for Single Thread Assembly

4.4 Time-Dependent Behavior

The model is similar to the linear and nonlinear, non-time dependent model in that it is based on a series of springs connected to nodes and solved as a matrix structural analysis problem. The difference between the static model and the time dependent model is that the time-dependent model incorporates a spring and dashpot in parallel, alternatively called a Kelvin [17], Kelvin-Voight [17], or Voight [17] model, between the free node on the bolt thread and a newly defined slave node. A schematic of the Kelvin model is shown in Figure 6.

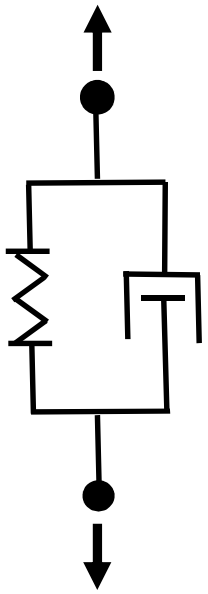

Figure 6. Schematic of Kelvin Model

In order to simulate the behavior of the Kelvin model a compressive force is applied to both ends. The spring is not compressed at all at first, so all of the load is carried by the dashpot. This initial load causes the dashpot to move. As the dashpot compresses, the spring also compresses and begins the carry some of the load as well as the dashpot. This reduces the rate of compression. Eventually, the spring has compresses sufficiently to carry all of the applied load, and the dashpot carries no load. At this point, the Kelvin model has reached a steady state, and will not compress any further,

The complete configuration of the time dependent model is shown in Figure 7. Each individual thread circumference is represented by a single Kelvin model in addition to the spring stiffness that was included in both the linear and nonlinear models presented previously. The numbering of the nodes is summarized in Table 7. The connectivity between the nodes is also shown in Figure 7, with the stiffnesses between nodes denoted by k_1 through k_4.

The Kelvin model allows the loss over time to be simulated. The dashpot introduces the dimension of time into the model. A dashpot behaves as a dampener and the rate of its compression is governed by a newly introduced variable. This variable has the units of kip-seconds per inch and relates the rate of compression of the dashpot, in units for distance per time, to the applied force. The spring that is parallel to the dashpot causes the force in the spring-dashpot mechanism to transfer to the spring as the dashpot compresses. This allows the dashpot to compress only a finite distance and as a result the force loss per time increment gradually slows under constant displacements. The spring in parallel with the dashpot is the object that holds the force that is loss in each time

increment. The entire spring-dashpot mechanism is used to reduce the force that is exerted on the springs that represent the stiffness of the point of contact between the bolt and nut threads. The result of this behavior is the simulation of relaxation in the bolt over a specified time period. The stiffnesses and dashpot constant are summarized in Table 7. For these tables, threads are numbered such that 1 is furthest from the clamped surface, n is closest to the clamped surface.

Table 7

Node Numbering for Model

Nodes	Description
$(1)_f \ldots (2i\text{-}1)_f \ldots (2n\text{-}1)_f$	Center line of bolt at i^{th} thread.
$2_f \ldots 2i_f \ldots 2n_f$	On the nut, corresponding to i^{th} thread.
$(2n+2+i)_d$	At thread POC, corresponding to i^{th} thread
$(2n+1)_s$	Center line of the bolt at the head.
$(2n+2)_s$	Boundary between nut and clamped plate.

The vector of slave node displacements, $\{U_d\}$, is written as,

$$\{U_d\} = [D]\{U_f\} + \{s\} \tag{30}$$

where [D] is the position matrix, $\{U_f\}$ are the free dislacements, and $\{s\}$ is a vector that describes the compression in the dashpots. The position matrix [D] identifies the free

nodes of the bolt threads that the displacements of the slave nodes are tied to, and takes the form

$$D = \begin{bmatrix} 1 & 0 & 0 & 0 & 0 & 0 & 0 & 0 & 0 & 0 \\ 0 & 0 & 1 & 0 & 0 & 0 & 0 & 0 & 0 & 0 \\ 0 & 0 & 0 & 0 & \ddots & 0 & 0 & 0 & 0 & 0 \\ 0 & 0 & 0 & 0 & 0 & 0 & 1 & 0 & 0 & 0 \\ 0 & 0 & 0 & 0 & 0 & 0 & 0 & 0 & 1 & 0 \end{bmatrix} \tag{31}$$

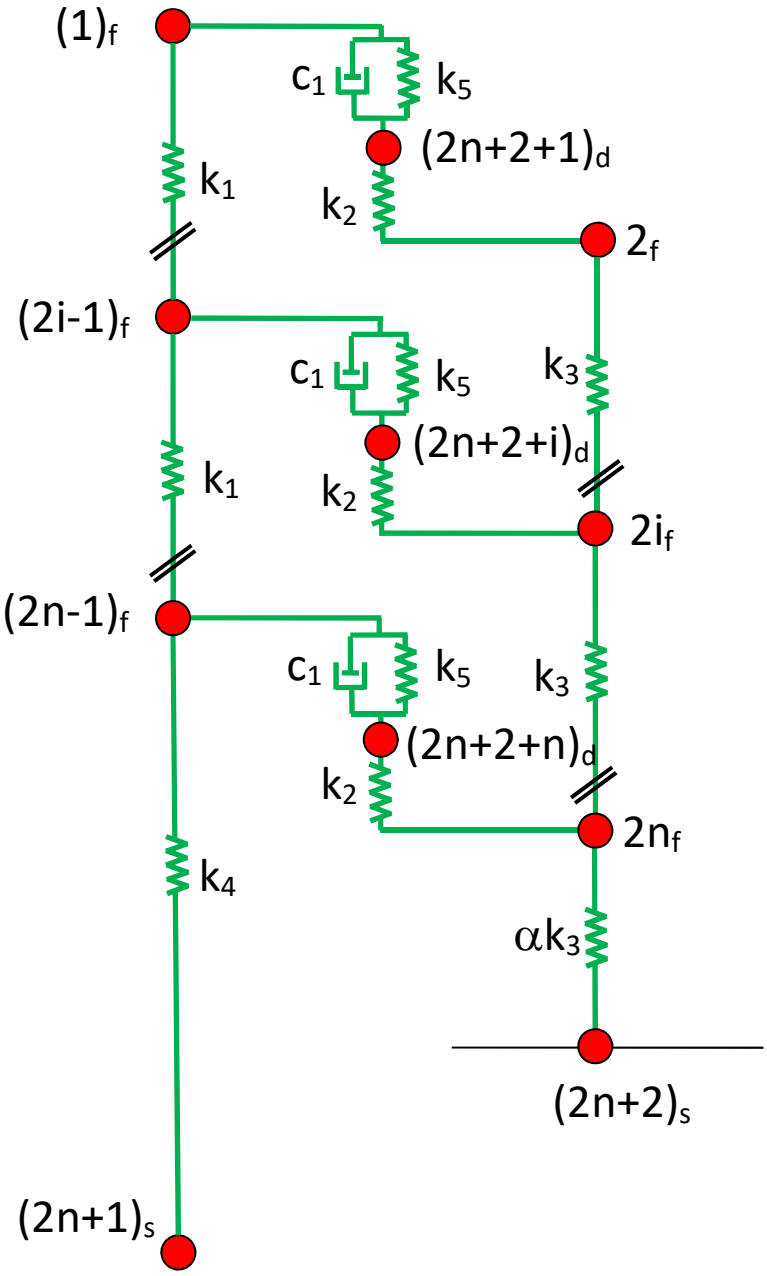

Figure 7. Bolt-Nut Assembly Schematic for Time Dependent Behavior

Table 8

Linear Elastic Constants Between Nodes

Stiffness	Connected Nodes	Description
k_1	$(2i-1)_f$ and $(2i-3)_f$	Stiffness of bolt between threads i and i-1.
k_2	$2i_f$ and $(2i-1)_f$	Stiffness of thread i.
k_3	$2i_f$ and $(2i-2)_f$	Stiffness of nut between threads i and i-1.
αk_3	$2n_f$ and $(2n+2)_s$	Stiffness of nut between n^{th} thread and clamped plate.
k_4	$(2n-1)_f$ and $(2n+1)_s$	Stiffness of bolt along effective clamped length.
k_5	$(2n+2+i)_d$ and $(2i-1)_f$	Stiffness of resistance to relaxation force
c_1	$(2n+2+i)_d$ and $(2i-1)_f$	Rate of relaxation constant at thread POC

The values of k_1 through k_4 and α were defined in a previous section. The value of k_5, like k_2 and k_3, was not determined through a solid mechanics approach, but rather from experimental data. This stiffness corresponds to the resistance to relaxation the bolt will display over time while c_1, which was also determined from experimental data, represents the rate at which that relaxation will occur.

The partitioned equilibrium equation is given by Equation 32.

$$\begin{Bmatrix} F_f \\ F_s \\ F_d \end{Bmatrix} = \begin{bmatrix} K_{ff} & K_{fs} & K_{fd} \\ K_{sf} & K_{ss} & K_{sd} \\ K_{df} & K_{ds} & K_{dd} \end{bmatrix} \begin{Bmatrix} U_f \\ U_s \\ U_d \end{Bmatrix} + \begin{bmatrix} C_{ff} & C_{fs} & C_{fd} \\ C_{sf} & C_{ss} & C_{sd} \\ C_{df} & C_{ds} & C_{dd} \end{bmatrix} \begin{Bmatrix} \dot{U}_f \\ \dot{U}_s \\ \dot{U}_d \end{Bmatrix} \tag{32}$$

The resulting stiffness submatrices are presented in Equations 33 through 38. Note that node numbering is such that the global stiffness matrix is readily partitioned into K_{ff}, K_{fs}, K_{sf}, K_{ss}, K_{fd}, K_{df}, K_{sd}, K_{ds}, and K_{dd}. A similar matrix, C, is defined for the dashpot constant. It is partitioned in a similar manner into C_{ff}, C_{fs}, C_{sf}, C_{ss}, C_{fd}, C_{df}, C_{sd}, C_{ds}, and C_{dd} and is given by Equation 39. It should also be noted that the partitioned submatrices K_{sd} and K_{ds} in Equation 37 are zero matrices. The partitioned submatrices C_{fs}, C_{sf}, C_{ss}, C_{sd}, and C_{ds} in Equation 39 are also all zero matrices.

Equation 33 shows submatrix K_{ff}.

$$K_{ff} = \begin{array}{c|cccccccc} & 1 & 2 & 3 & 4 & \cdots & 2n-2 & 2n-1 & 2n \\ \hline 1 & k_1 + k_5 & 0 & -k_1 & & & & & \\ 2 & 0 & k_2 + k_3 & 0 & -k_3 & & & & \\ 3 & -k_1 & 0 & 2k_1 + k_5 & 0 & \ddots & & 0 & \\ 4 & & -k_3 & 0 & k_2 + 2k_3 & 0 & \ddots & & \\ \vdots & & & \ddots & 0 & \ddots & \ddots & \ddots & \\ 2n-2 & & 0 & & \ddots & \ddots & k_2 + 2k_3 & 0 & -k_3 \\ 2n-1 & & & & & \ddots & 0 & k_1 + k_4 + k_5 & 0 \\ 2n & & & & & & -k_3 & 0 & k_2 + (1+\alpha)k_3 \end{array}$$

(33)

Equation 34 shows submatrix K_{fs} . Note that $K_{sf} = K_{fs}^{T}$.

$$K_{fs} = \begin{array}{c|cc} & 2n+1 & 2n+2 \\ \hline 1 & & \\ 2 & & \\ 3 & & \\ & 0 & \\ 4 & & \\ \vdots & & \\ 2n-2 & & \\ \hline 2n-1 & -k_4 & \\ \hline 2n & 0 & -\alpha k_3 \end{array}$$

(34)

Equation 35 shows submatrix K_{fd}. It should be noted that $K_{df} = K_{fd}^{T}$.

$$K_{fd} = \begin{array}{c|ccc} & 2n+2+1 & 2n+2+i & 2n+2+n \\ \hline 1 & -k_5 & & \\ 2 & -k2 & & \\ 3 & & \ddots & 0 \\ 4 & & \ddots & \\ \vdots & & \ddots & \ddots \\ 2n-2 & 0 & \ddots & 0 \\ 2n-1 & & & -k_5 \\ 2n & & & -k_2 \end{array}$$

(35)

Equation 36 shows submatrix K_{ss}.

$$K_{ss} = \begin{array}{c|cc} & 2n+1 & 2n+2 \\ 2n+1 & k_4 & 0 \\ 2n+2 & 0 & \alpha k_3 \end{array}$$

(36)

Equation 37 shows submatrix K_{sd}. It should be noted that $K_{ds} = K_{sd}^{T}$.

$$K_{sd} = \begin{array}{c|ccc} & 2n+2+1 & 2n+2+i & 2n+2+n \\ 2n+1 & & & \\ & & 0 & \\ 2n+2 & & & \end{array}$$

(37)

Equation 38 shows submatrix K_{dd}.

$$K_{dd} = \begin{array}{c|ccc} & 2n+2+1 & 2n+2+i & 2n+2+n \\ 2n+2+1 & k_5+k_2 & 0 & \\ 2n+2+i & & \ddots & \\ 2n+2+n & & 0 & k_5+k_2 \end{array}$$

(38)

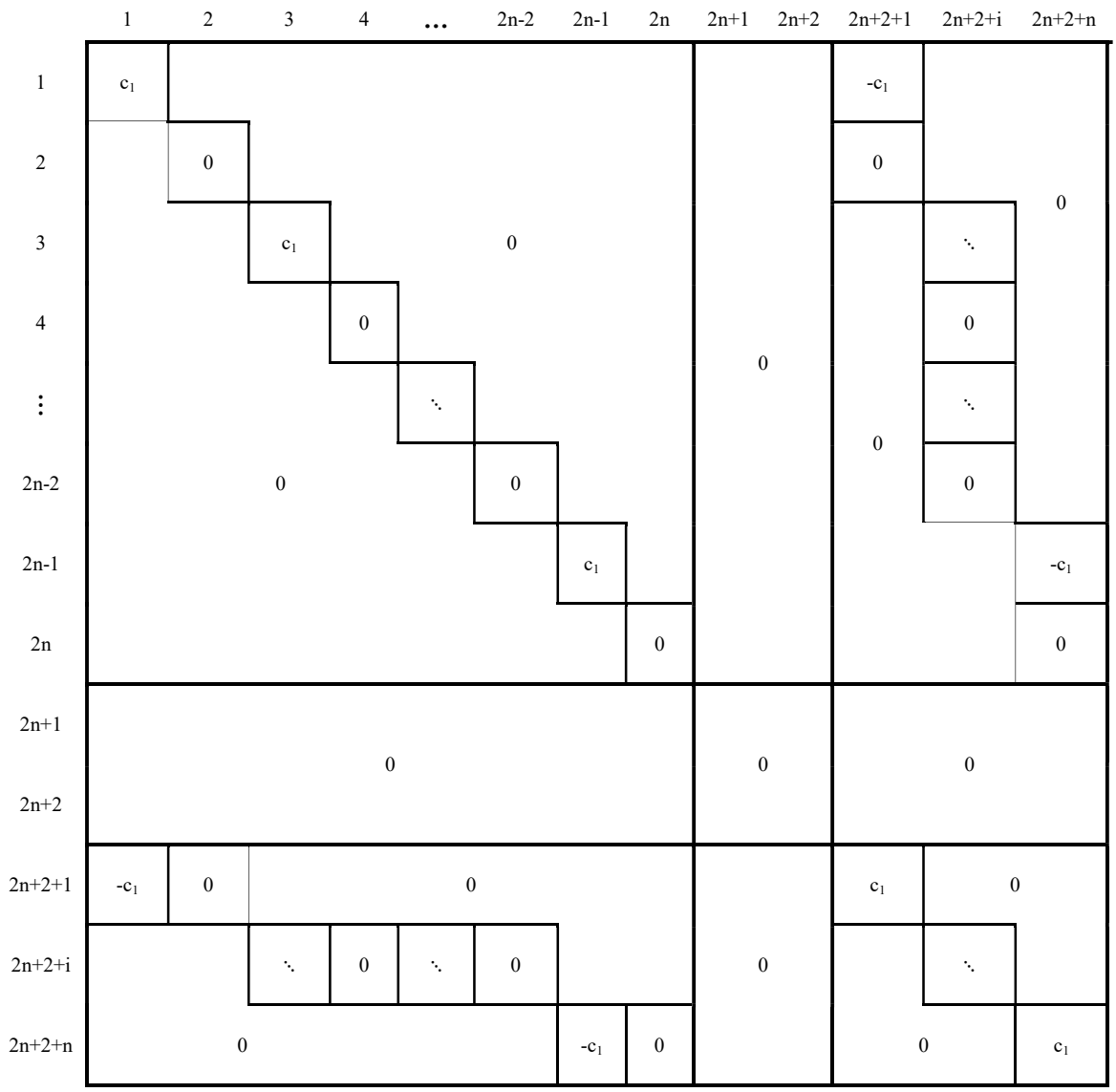

(39)

In practice, in the same application as in the linear elastic case, tension is applied to a bolt by turning the nut. This reduces the pre-strained length of the bolt that spans the grip length. Rather than shortening the gripped length, tightening is simulated in the model by displacing the node at the head of the bolt by a distance

$$u_{(2n+1)_s} = \frac{-p\theta}{2\pi} \tag{40}$$

where, p is the pitch of the thread and θ is the rotation of the nut from the zero force position, measured in radians. Note that the model assumes linear behavior starting immediately from some baseline zero rotation. This is not the actual behavior observed in practice, rather a linear region is observed after a small, initial rotation. The second displacement-specified node, 2n+2, is assumed to have zero displacement, resulting in a specified displacement vector which can be written as

$$\{U_s\} = \begin{Bmatrix} u_{(2n+1)_s} \\ u_{(2n+2)_s} \end{Bmatrix} = \begin{Bmatrix} \frac{-p\theta}{2\pi} \\ 0 \end{Bmatrix} \tag{41}$$

As there are no external forces applied, *i.e.*, $\{F_f\} = 0$, Equation 32 may be re-written to solve for the vector of free displacements. In the case of time dependent behavior, solving for the vector of free displacements is not as straightforward as it is with the static simulation. From Equation 32, and noting that $[C_{fs}] = [0]$, F_f can be equated to

$$\{0\} = \{F_f\} = [K_{ff}]\{U_f\} + [K_{fs}]\{U_s\} + [K_{fd}]\{U_d\} + [C_{ff}]\{\dot{U}_f\} + [C_{fd}]\{\dot{U}_d\} \tag{42}$$

Likewise, there are no forces applied at the slave nodes, so $\{F_d\} = \{0\}$, and noting that $[K_{ds}]$ and $[C_{ds}]$ are zero matrices, Equation 32, can be re-written to solve for the velocity vector of the slave nodes.

$$\{0\} = \{F_d\} = [K_{df}]\{U_f\} + [K_{dd}]\{U_d\} + [C_{df}]\{\dot{U}_f\} + [C_{dd}]\{\dot{U}_d\} \quad (43)$$

Enforcing $\{F_d\}$ to $\{0\}$, and considering Equation 32 results in

$$\{0\} = [K_{df}]\{U_f\} + [K_{dd}]\big[[D]\{U_f\} + \{s\}\big] + [C_{df}]\{\dot{U}_f\} + [C_{dd}]\{\dot{U}_d\} \quad (44)$$

We can now solve for $\{\dot{U}_d\}$

$$\{\dot{U}_d\} = -[C_{dd}]^{-1}\big[[K_{df}] + [K_{dd}][D_1]\big]\{U_f\} - [C_{dd}]^{-1}[K_{dd}]\{s\} - [C_{dd}]^{-1}[C_{df}]\{\dot{U}_f\} \quad (45)$$

Equation 30 and 45 can now be substituted into Equation 42 to solve for the vector of free displacements. As Equation 45 is simplified it can be seen that

$$\begin{aligned}\{0\} = \big[[K_{ff}] + [K_{fd}][D]\big]\{U_f\} + [K_{fd}]\{s\} + [K_{fs}]\{U_s\} + [C_{ff}]\{\dot{U}_f\} \\ - [C_{fd}][C_{dd}]^{-1}\big[[K_{df}] + [K_{dd}][D]\big]\{U_f\} - [C_{fd}][C_{dd}]^{-1}[K_{dd}]\{s\} \\ - [C_{fd}][C_{dd}]^{-1}[C_{df}]\{\dot{U}_f\}\end{aligned} \quad (46)$$

We find that

$$[C_{ff}] - \big[[C_{fd}][C_{dd}]^{-1}[C_{df}]\big] = 0 \quad (47)^{[1]}$$

[1] See Appendix A.

Based on the results of the matrix algebra in Equation 47, we can further simplify Equation 46 to

$$0 = \left[[K_{ff}] + [K_{fd}][D] - [C_{fd}][C_{dd}]^{-1}\left[[K_{df}] + [K_{dd}][D]\right]\right]\{U_f\} + \left[[K_{fd}] - [C_{fd}][C_{dd}]^{-1}[K_{dd}]\right]\{s\} + [K_{fs}]\{U_s\} \quad (48)$$

Solving for $\{U_f\}$ gives us the vector of free displacements as defined by

$$\{U_f\} = \left[[K_{ff}] + [K_{fd}][D] - [C_{fd}][C_{dd}]^{-1}\left[[K_{df}] + [K_{dd}][D]\right]\right]^{-1}\left[\left[[C_{fd}][C_{dd}]^{-1}[K_{dd}] - [K_{fd}]\right]\{s\} - [K_{fs}]\{U_s\}\right] \quad (49)$$

Once the free displacements are found, the load transfer by the i^{th} thread (numbered with 1 as the furthest from the clamped surface and n as the closest to the clamped surface), F_i, is given by

$$F_i = k_2\left(u_{2i} - u_{2i-1} - s_{i,total}\right) \quad (50)$$

By subtracting the total displacement in the dashpot from the free displacements as time increases a loss in force will begin to occur. The force in the bolt is given by

$$F_{n+1} = k_4(u_{2n+1} - u_{2n-1} - s_n) \quad (51)$$

4. 4. 1 Simulation of losses over time. Now that the free displacements as a function of the governing time dependent parameters, k_5 and c_1, are known, a way to simulate the occurring losses must be determined. To do this we use

$$\{\dot{U}_d\} = [D]\{\dot{U}_f\} + \{\dot{s}\} \tag{52}$$

where $\{\dot{U}_d\}$ represents the rate at which the slave nodes are moving which is simulated by $\{\dot{s}\}$ which is a vector describing the rate at which each dashpot compresses. This rate, $\{\dot{s}\}$, must be solved for to obtain an initial velocity of the slave nodes when time is equal to 0. From this point the simulation steps through using time intervals from $\{\dot{s}\}$ which is recalculated after each step. Based on the mechanics of the dashpot, the rate $\{\dot{s}\}$ will decrease over time until it reaches a point in time where the individual threads are no longer is losing force. Therefore, the bolt will have reached a steady state loading condition. To implement this behavior, Equation 52 is substituted into Equation 43 to obtain,

$$\{0\} = [K_{df}]\{U_f\} + [K_{dd}]\{U_d\} + [C_{df}]\{\dot{U}_f\} + [C_{dd}][D]\{\dot{U}_f\} + [C_{dd}]\{\dot{s}\} \tag{53}$$

Upon observation,

$$[C_{df}]\{\dot{U}_f\} + [C_{dd}][D]\{\dot{U}_f\} = 0 \tag{54}$$[2]

simplifying the equation to

[2] See Appendix B.

$$\{0\} = [K_{df}]\{U_f\} + [K_{dd}]\{U_d\} + [C_{dd}]\{\dot{s}\} \quad (55)$$

The dashpot compression rate can be solved and Equation 30 can be inserted into Equation 55 thus giving,

$$\{\dot{s}\} = [C_{dd}]^{-1}\left[[K_{df}]\{U_f\} + [K_{dd}]\left[[D]\{U_f\} + \{s\}\right]\right] \quad (56)$$

The simulation then steps through time increments to simulate the relaxation behavior until compression is no longer being lost in the bolt. A correctly calibrated simulation should produce output that fits well with experimentally observed data.

4. 4. 2 Calibration of independent parameters. The model has two previously undetermined, independent parameters which relate to the mechanical properties of the bolt, k_5 and c_1. These two parameters govern how much loss occurs over time. During elastic behavior these parameters govern the model as follows. It can be assumed that when time is equal to 0, the vector of free displacements, $\{U_f\}$, is the same as under non-time dependent conditions. To simulate this condition, the model starts when $\{s\} = 0$. Since no time has passed $\{s\}$ must be zero because $\{s\}$ is defined as the displacement in the dashpot. We are left with the initial free displacements found from the non-time dependent, linear elastic model. However, it is not possible to calibrate when time is equal to zero because regardless of the values of k_5 and c_1, the initial displacements of the threads will remain the same. This is to be expected of the model.

What is known is the $\{\dot{s}\}$ vector, which can allow the model to step through any length of time increment using any values for k_5 and c_1. It is also important to understand that, while k_5 and c_1 are independent of the previously determined stiffnesses, they are also independent of each other. This creates a practical calibration process. First, k_5 can be calibrated until the losses that occur in the simulation compare well to those determined experimentally. Once the desired losses are found, c_1 can be calibrated until those losses occur over the length of time that was observed experimentally.

Upon observation of Equation 56 it is apparent that the rate of compression in the dashpot will not change based on the applied force of the initial pretension. To simulate this observed behavior it is necessary to implement a threshold method within the simulation that controls the rate based on the pretension.

The trend line of the plotted experimental data is best represented as linear. Figure 8 below displays this data [18].

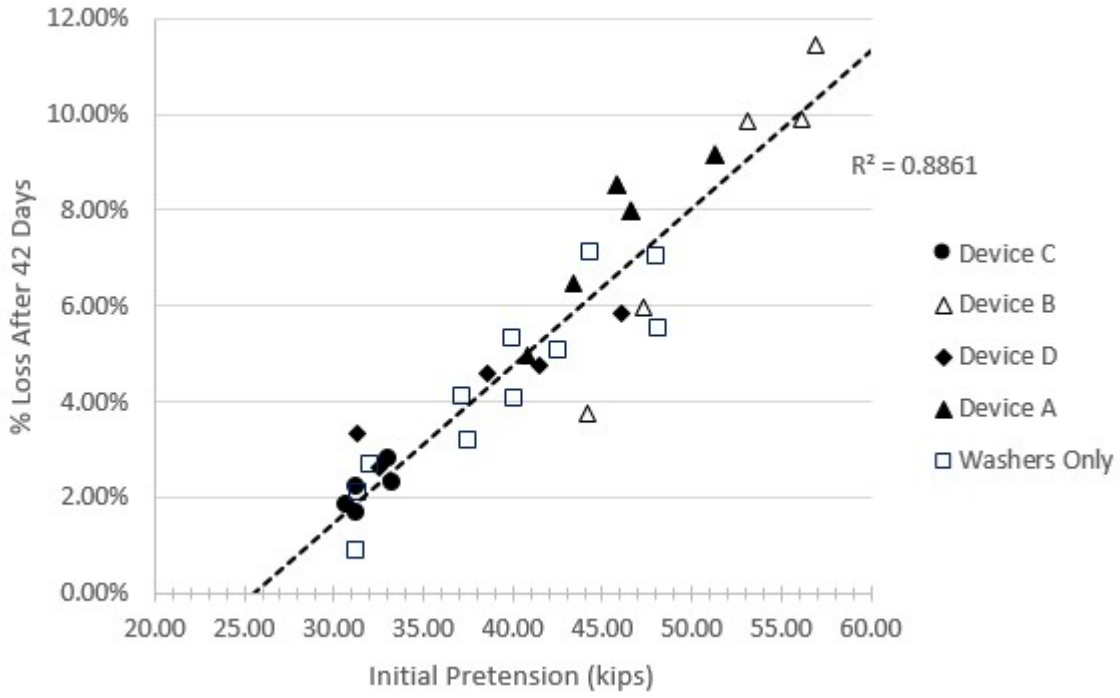

Figure 8. Experimental Relaxation Data [9]

Using the equation of the trend line, the value at which no losses occur was determined. This pretension was the threshold and all simulated losses for any given bolt could be scaled linearly based on this limit to achieve the correct behavior within the model. It has previously been determined experimentally relaxation is governed primarily by the initial pretension. Variations in hardware and bolt type had little effect on the amount of observed losses for a single bolt size [9]. The experimental work done of time dependent losses focused on a 7/8 inch diameter bolt. Therefore, the use of a single threshold value is sufficient within the model as there was insufficient relaxation data from a 3/4 inch

diameter bolt to make a reasonable comparison between the simulation and what was observed experimentally.

Upon observation of Equation 56, which gives the rate of compression in the dashpot, the equation can be viewed as the inverse of the slave-node, damping coefficient sub-matrix multiplied by a force vector. The threshold must be subtracted from that force at every time step to scale the relaxation at varying pretensions. At the end of every time step the model does a check to make sure that negative values of load distribution on the threads are excluded from the total force in the bolt. Implementing this behavior resulted in larger losses as the pretension was increased. Once the correct behavior was obtained, k_5 and c_1 were calibrated separately until the correct losses occurred over the correct period of time.

Chapter 5

Numerical Results and Discussion

5.1 Linear Elastic Model

Using the calibrated k_2 and k_3 values for the 3/4 in. diameter and 7/8 in. diameter bolts (based on single-thread tests), the remaining stiffness values were found using the numeric simulation for elastic bolt behavior. The simulation was run multiple times for each diameter bolt to find numerical stiffness values representative of any given number of engaged threads for that size. The output is depicted in Figures 8 and 9 for the 3/4 in. and 7/8 in. bolts, respectively, and is plotted against the experimentally determined stiffness values. The fit for both diameter bolts is good with the 3/4 in. bolt matching especially well. It should be noted that the dashed lines in Figures 9 and 10 represent the stiffnesses using values of beta ±0.02 from the calibrated values. The upper line is +0.02 beta and the lower line is -0.02 beta for both Figures 9 and 10.

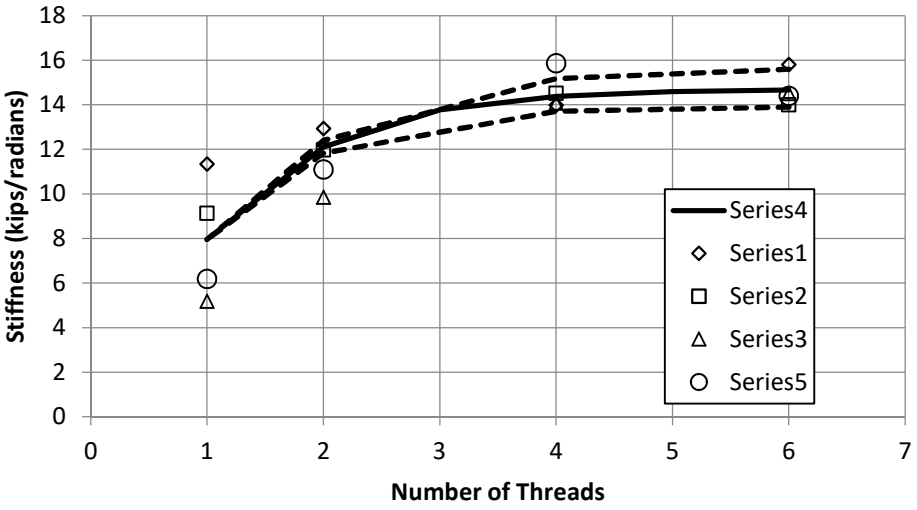

Figure 9. Experimental vs. Numerical Stiffnesses – 3/4 in. Bolt

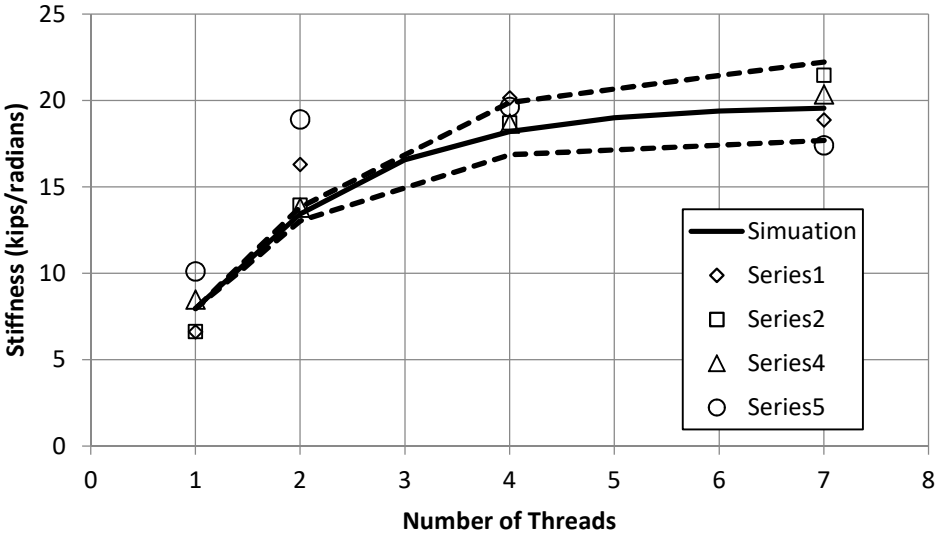

Figure 10. Experimental vs. Numerical Stiffnesses – 7/8 in. Bolt

5.2 Non-Linear Model

After running the simulation using the calibrated k_2 and k_3 values as an elastic analysis, the simulation was then ran using the same k_2 and k_3 values as an analysis of elastic-

plastic behavior. The experimentally determined values for single thread yield in 3/4 in. and 7/8 in. diameter bolts were 11 kip and 10 kip, respectively. Using these values in conjunction with the calibrated spring stiffnesses, the simulation method described in Section 4.4.1 was implemented. The output is depicted in Figures 11 and 12 for the 3/4 in. and 7/8 in. bolts, respectively, and is plotted against the experimentally recorded force versus rotation values. The large points along the simulation line represent when, in the simulation, the threads yielded. Again, the fit is good for both bolt diameters. However, as was also the case with elastic behavior, the 3/4 in. diameter bolt plot has a better fit.

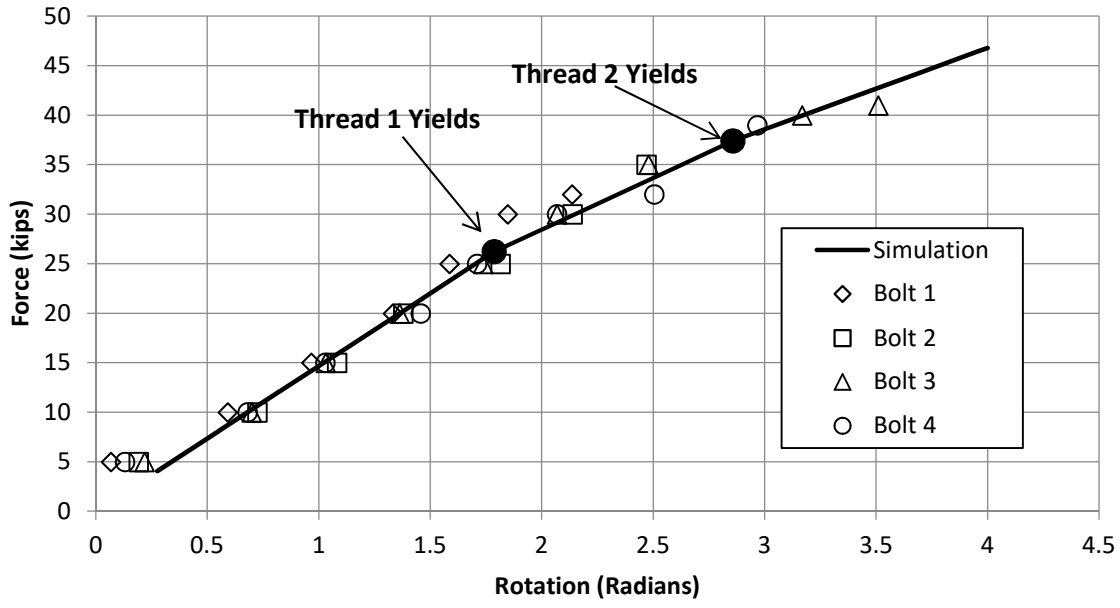

Figure 11. Non-Linear Behavior - 3/4 in. Bolt

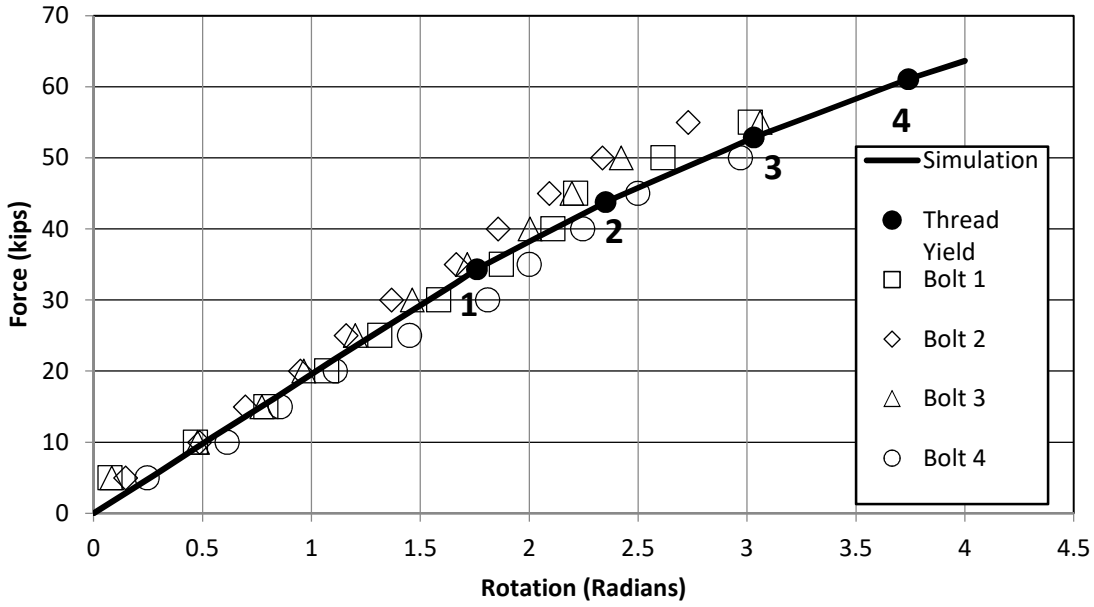

Figure 12. Non-Linear Behavior – 7/8 in. Bolt

Many previous studies have determined the load distribution on the threads in a linear elastic bolt model. As observed by Sopwith [3], accounting for nonlinear behavior in the threads results in a more uniform distribution of load across the length of the thread. The load distribution on the threads as predicted by the nonlinear model as the load is increased is shown in Figures 13 and 14 for the 3/4 in. and 7/8 in. bolts, respectively. In both plots, it is apparent at what force a thread yields. Once a thread yields the remaining threads take most of the increasing load until another thread yields and this behavior continues until the entire bolt yields.

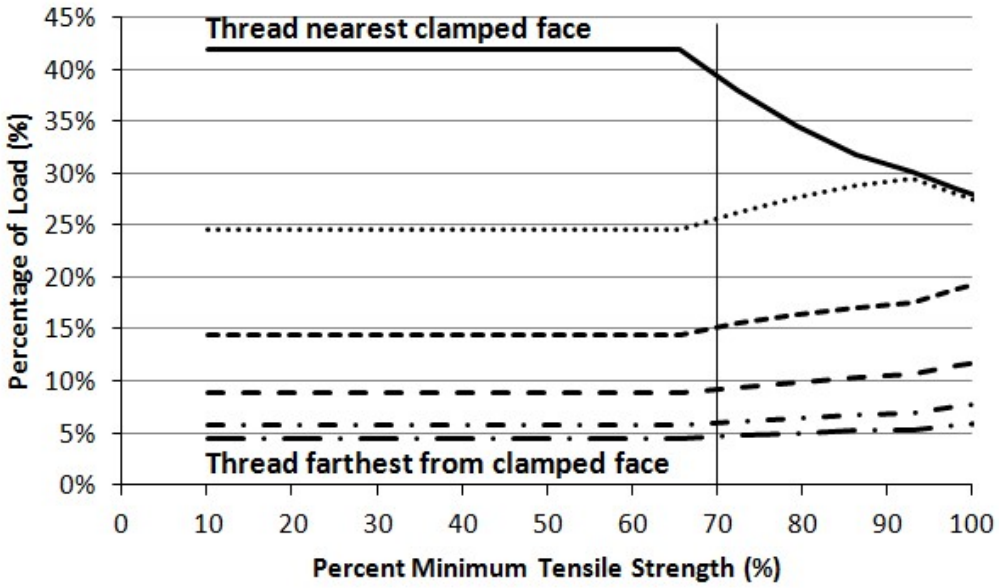

Figure 13. Thread Load Distribution – 3/4 in. Bolt

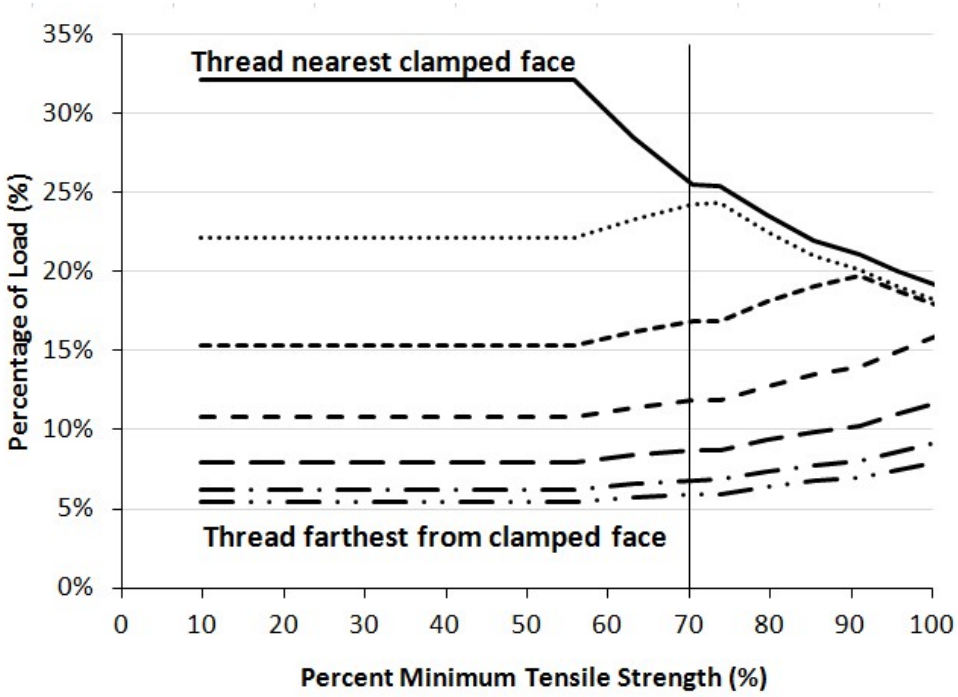

Figure 14. Thread Load Distribution – 7/8 in. Bolt

Comparisons can be made between Figure 14 to Miller, Figure 7 [4], which shows the percent of the total load on each thread for a one inch diameter steel bolt. The figure plots photoelastic [2], theoretical [3], and spring model results [4]. When comparing this data which has been reproduced in Figure 15, the percent of the total load on each thread is similar. Based on these observations, it can be concluded that the calibration process of the independent variables in the model was accurate.

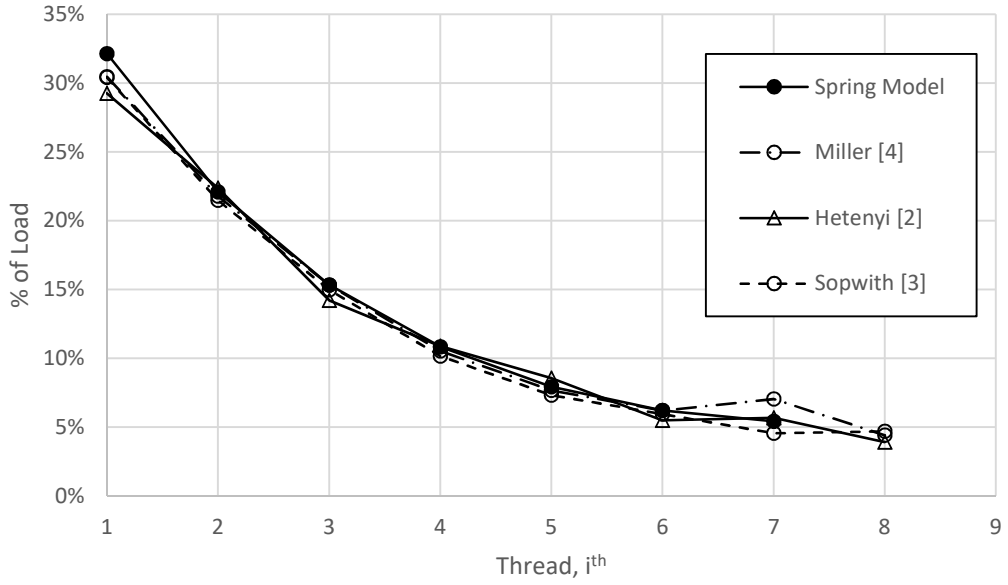

Figure 15. Thread Load Distribution Comparison

5.3 Time Dependent Model

Using the calibrated k_5 and c_1 values, the simulation was run using the same pretension values based on the trend observed during testing. The results at each initial pretension were then plotted against the experimental data plotted in Figure 16 for 7/8" diameter bolts.

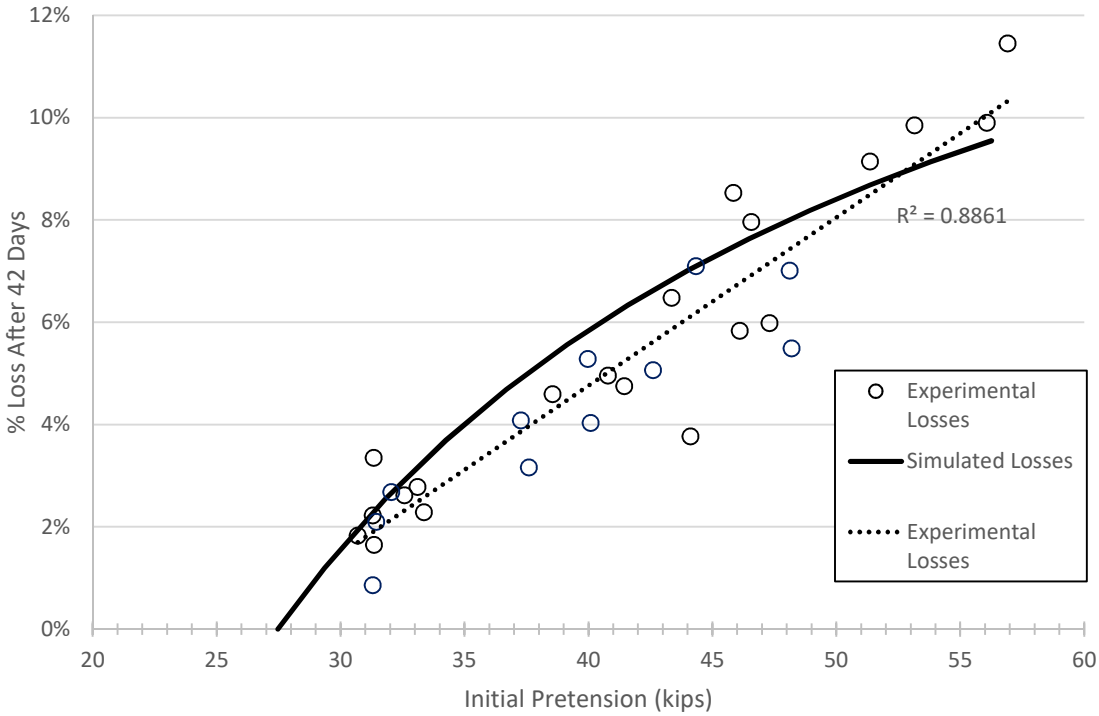

Figure 16. Experimental vs. Simulated Losses - 7/8 in. Bolt

The comparison between the experimental and simulated losses is good. The increasing simulated losses follow a curved trend as a result of the implemented threshold to scale the relaxation behavior. Based on the difference between the trend observed experimentally and the simulated losses, it is possible that, at higher loads, the

experimental losses could begin to exhibit the same trend as the simulation. Due to the range of pretensions used in this study additional testing would be required.

Chapter 6

Conclusions & Recommendations

This research focused on the relaxation in bolted assemblies. In order to effectively simulate this behavior models were developed to simulate the relaxation in the bolts. Results of these models predict the load distribution on the threads under elastic and plastic conditions. Models such as these have been developed in previous research. The spring model this research focused on differs from previous works because it used a pretension based on an initial rotation to determine the load on each thread. The length of the bolt shank was also used to develop a corresponding stiffness. In this scenario the force in the bolt was then a function of the initial rotation and the subsequent displacement in the shank from its original length based on that rotation. The capability to simulate displacement in the bolt shank was significant because the model could then be extended to incorporate the element of time where displacements would vary based on the time increment. This was the plastic deformations that created the losses which occurred in the bolt.

6.1 Summary of Findings

The findings from the analysis described in this thesis are summarized below.

6. 1. 1 Linear elastic behavior. The load distribution on the threads of bolted-assemblies under linear elastic conditions has been extensively researched in the past. However, for the purposes of studying time-dependent behavior it has proved necessary to the calibration of the independent parameters used to determine the stiffnesses that are specific to the material and geometric properties of the bolts used in the study. The

values of the k_2 and k_3 stiffnesses were functions of the dimensionless parameter, β. This value was determined by incrementing its value and comparing the simulated stiffness to that found based on experimental data. The results of this incremental approach found β to be 0.872 for the ¾ inch dimeter bolt and 0.933 for the 7/8 inch diameter bolt. Using these β values, the actual spring stiffnesses, k_2 and k_3, could be found. These stiffnesses, as well as k_1 and k_4, which were known *a priori* through a solid-mechanics approach, are summarized in the following table.

Table 9

Stiffnesses of ASTM A325 Bolts

	3/4" Diameter A325 Bolt Stiffness (kips/radians)	**7/8" Diameter A325 Bolt Stiffness** (kips/radians)
k_1	9,694. 4	12,200
k_2	635. 62	520. 77
k_3	2,165. 1	3,626. 0
k_4	5,147. 4	7,163. 4

The values were verified after the results of the simulated load distribution on the threads compared well with the experimentally determined distribution. These stiffness values were then used in the other models covered in this paper; the non-linear model and the time dependent model.

6. 1. 2 Non-linear behavior. Using the determined stiffness values a non-linear analysis was run to determine how much incorporating thread yielding behavior lead to a better comparison to the experimental results. The results of this simulation showed that thread yielding allows for a better comparison which could lead to better development of a non-linear, time-dependent model.

6. 1. 3 Time dependent behavior. The same thread stiffnesses were used in the linear elastic time dependent model. This model was extended to include the simulation of the observed relaxation behavior. Two additional independent parameters were calibrated as well, k_5 and c_1. These were modelled in parallel to add the additional time dimension to the model. The values for k_5 and c_1 were 714 kips/inch and 60,000 kip-hours/inch. Once calibrated, the simulation results compared well with the experimentally determined losses, though slightly higher.

6.2 Conclusions

Each model compared well with the experimental results once the independent parameters were calibrated. The difference between the losses of the linear elastic, time – dependent simulation and the experimental values could be attributed to not accounting for plastic behavior in the time-dependent model. The decrease in thread stiffness due to yielding could lessen the difference in the results.

6.3 Recommendations

The results and conclusions of this thesis can most immediately be extended into the development of a relaxation simulation that incorporates elastic-plastic behavior to determine whether this leads to a better comparison with the experimental results. Relaxation testing using a wider variety of bolt diameters and lengths is recommended to

further determine the accuracy of the simulation. Expanding the model to be applied to any type of bolt would require more tests to determine potential variables to incorporate as the diameter and lengths change. Additional testing at higher pretensions is also recommended. This would enable a determination of whether experimental losses will continue to exhibit a linear trend or whether they will start to follow the curve resulting from the simulated output. Additionally the results of this thesis can be used as an additional comparison resource for future finite element models of the same A325 high-strength bolt assemblies. The greater the amount of available data will lead to a better understanding of the relaxation behavior.

References

[1] Goodier, J., "The Distribution of Load in the Threads of Screws," Journal of Applied Mechanics, pp. 10-16, 1940.

[2] Hetenyi, M., "The Distribution of Stress in Threaded Connections," Experimental Stress Analysis: Proceedings of the Society for Experimental Stress Analysis, pp. 147-156, 1943.

[3] Sopwith, D., "The Distribution of Load in Screw Threads," Proceedings of the Institute of Mechanical Engineers, Vol. 159, pp. 373-383, 1948.

[4] Miller, D., Marshek, K., Naji, M., "Determination of Load Distribution in a Threaded Connection," Mechanism and Machine Theory, Vol. 18, No. 6, pp. 421-430, 1983.

[5] Curti, G., Raffa, F., "A Simplified Study on the Load Distribution on Threads of Compression and Tension Nuts," Wire, Vol. 38, Issue 3, pp. 334-338, 1988.

[6] Wang W., Marshek, K., "Determination of Load Distribution in a Threaded Connector with Yielding Threads," Mech. Mach. Theory, Vol. 31, No., pp. 29-244, 1996.

[7] Fukuoka, T., Takaki, T., "Evaluation of the Tightening Process of Bolted Joint with Elastic Angle Control Method," Analysis of Bolted Joints, Vol. 478, pp. 11-18, 2004.

[8] E. Chesson, W. Munse, Studies of the Behavior of High-Strength Bolts and Bolted Joints, Bulletin 469, pp.1-34, 1965.

[9] D. Reuther, Baker, I., Yetka, A., D. Cleary, W. Riddell,. Relaxation of ASTM A325 Bolted Assemblies, Journal of Structural Engineering, 2014.

[10] Yang J., DeWolf J., Mathematical Model for Relaxation in High-Strength Bolted Connections, Journal of Structural Engineering, pp. 803-809, 1999.

[11] Oostdyk, Matthew et al., Time dependent behavior of a FRR thermal break pad under compressive loads, Structure , Volume 2, 44 – 49, 2014.

[12] Maruyama, K., "Stress Analysis of a Bolt-Nut Joint by the Finite Element Method and Copper-Electroplating Method," Bul. JSME, Vol. 17, No. 106, pp. 442-450, 1974.

[13] Tanaka M., Miyazawa, H., Asaba, E., Hongo K., "Application of the Finite Element Method to Bolt-nut Joints – Fundamental Studies on Analysis of Bolt-nut Joints," Bulletin of the JSME, Vol. 24, No. 192, pp. 1064-1071, 1981.

[14] Joanovics, L., Varadi, K., "Nonlinear Finite Element Analysis of the Contact, Strain, and Stress States of a Bolt-Nut-Washer-Compressed Sheet Joint System," Periodica Polytechnica Ser. Mech. Eng, Vol. 39, No. 2, pp. 151-162, 1995.

[15] ASTM E797 / E797M-15, Standard Practice for Measuring Thickness by Manual Ultrasonic Pulse-Echo Contact Method, ASTM International, West Conshohocken, PA, 2015, www.astm.org

[16] Research Council on Structural Connections. (2009). Specification for structural joints using high-strength bolts, American Institute of Steel Construction.

[17] Shames, Irving H. *Engineering Mechanics: Statics and Dynamics: Instructor's Manual*. Englewood Cliffs, N.J: Prentice-Hall, 1980. Print.

Appendix A

Proof – Show that $[C_{fd}][C_{dd}]^{-1}[C_{df}] = [C_{ff}]$

$$[D] = \begin{bmatrix} 1 & 0 & 0 & \cdots & & & 0 \\ 0 & & 1 & 0 & & & \\ \vdots & & & & \ddots & & \\ & & & & & & \\ 0 & & & & & 1 & 0 \end{bmatrix}$$

$D_{ij} = 1$ if $j = 2i - 1$
= 0 otherwise

$$[C_{ff}] = \begin{bmatrix} C_1 & 0 & \cdots & & 0 \\ 0 & 0 & & & \\ \vdots & & C_1 & 0 & \\ & & & \ddots & \\ & & 0 & & \\ & & & 0 & \\ 0 & & & & C_1 \end{bmatrix}$$

$C_{ff} = C_1$ if $i = 2k - 1$
For k = 1 .. n
= 0 otherwise

$$[C_{fd}] = \begin{bmatrix} -C_1 & 0 & \cdots & 0 \\ 0 & 0 & & \\ \vdots & -C_1 & & \\ & 0 & & \\ & & \ddots & \\ & & & -C_1 \\ 0 & & & 0 \end{bmatrix}$$

$C_{fd_{ij}} = -C_1$ if $i = 2j - 1$
= 0 otherwise

$$[C_{df}] = \begin{bmatrix} -C_1 & 0 & 0 & \cdots & & & 0 \\ 0 & & -C_1 & 0 & & & \\ \vdots & & & & \ddots & & \\ & & & & & & \\ 0 & & & & & -C_1 & 0 \end{bmatrix}$$

$C_{df_{ij}} = -C_1$ if $j = 2i - 1$
= 0 otherwise

$$C_{dd}{}^{-1}{}_{ij} = \frac{1}{C_1} \text{ if } i = j$$

0 otherwise

Consider $[C_{dd}]^{-1}[C_{df}]$

$$\begin{bmatrix} \frac{1}{C_1} & & & \\ & \frac{1}{C_1} & & \\ & & \ddots & \\ & & & \frac{1}{C_1} \end{bmatrix} \begin{bmatrix} -C_1 & 0 & \cdots & 0 \\ 0 & 0 & -C_1 & \\ \vdots & & \ddots & \\ 0 & & & -C_1 \quad 0 \end{bmatrix}$$

$$[C_{dd}]^{-1}[C_{df}]_{ij} = \sum_{l=1}^{n} C_{dd}{}^{-1}{}_{il} \cdot C_{df_{lj}}$$

The multiplication term

$$C_{dd}{}^{-1}{}_{il} \cdot C_{df_{lj}} = -1 \text{ if } i = l \text{ and } j = 2l - 1$$
$$= 0 \text{ otherwise}$$

$$[C_{dd}]^{-1}[C_{df}]_{ij} = -1 \text{ if } j = 2i - 1$$
$$= 0 \text{ otherwise}$$

$$\begin{bmatrix} -1 & 0 & 0 & \cdots & & & 0 \\ 0 & & -1 & 0 & & & \\ \vdots & & & & \ddots & & \\ & & & & & & \\ 0 & & & & & -1 & 0 \end{bmatrix}$$

Consider $[C_{fd}][C_{dd}]^{-1}[C_{df}]_{ij}$

$$= \sum_{m=1}^{n} C_{fd_{im}} \cdot {C_{dd}}^{-1} \cdot C_{df_{mj}}$$

$C_{fd_{im}} \cdot {C_{dd}}^{-1} \cdot C_{df_{mj}} = C_1$ if $i = 2m - 1$
and j = 2m-1

= 0 otherwise

Therefore

$$\sum_{m=1}^{n} C_{fd_{im}} \cdot {C_{dd}}^{-1} \cdot C_{df_{mj}} = 1 \text{ if } i = j$$

and i, j are odd
(or i = j = 2m-1 for m = 1,2,….n)

Appendix B

Proof – Show that $[\mathbf{C_{df}}] + [\mathbf{C_{dd}}][\mathbf{D}] = \mathbf{0}$

Note that: $C_{df_{ij}} = -c_1$ if $i = 2j - 1$
$= 0$ otherwise

$C_{dd_{ij}} = c_1$ if $i = j$
$= 0$ otherwise

$D_{ij} = 1$ if $i = 2j - 1$
$= 0$ otherwise

Now $[C_{dd}][D]_{ij} = \sum_{k=1}^{2n} C_{dd_{ik}} \cdot D_{kj}$

The terms will be zero unless both $C_{dd_{ik}}$ and D_{kj} are non-zero.

This only occurs when i = k and k = 2j – 1. So if i = 2j-1, $C_{dd_{ik}} D_{kj} = +c_1$

Which is the opposite of $C_{df_{ij}}$.

Appendix C

Simulation Code

```
%{ This file was really just used for calibrating beta for both diameter bolts.
%Thats what the while loop accomplished. Using the experimentally determined stiffnesses it loops
%the value of beta until a certain percent difference (a) was achieved. I ran this for different
%numbers of engaged threads for both both sizes. Those plots are in the paper. The first part is
%is material properties, constants, bolt dimensions and defining the matrices. Uf and Fm
%find the displacements then the forces.
%}

disp(' ')
%
prompt = 'Press 1 for 7/8" diameter and 2 for 3/4" diameter: ';
%
result = input(prompt);

if (result == 1)
  n = 7;
  d = 7/8.0;
  pitch = 0.11;
  slope = 7.966;
  lclamp = 1.96;
  shank = 1.88;
  % Full thread (7) experimental stiffness value for 7/8"
  stiffness=19.5295;
else
  n = 6;
  d = 3/4.0 ;
  pitch = 0.10;
  slope = 7.963775;
  lclamp = 2.07;
  shank = 2.00;
  % Full thread (6) experimental stiffness value for 3/4"
  stiffness = 14.6785;
end


%
E = 29000;
pi= 3.14159265359;
alpha = 2.00;
ashank = pi*d^2/4.0;
athread = 0.785*(d-0.9743*pitch)^2;
anut = pi*((d+0.25)^2-d^2)/4.0;
%
k1 = athread*E/pitch;
k4 = 1/(1/(alpha*k1)+shank/(ashank*E)+(lclamp-shank+d/3)/(athread*E));
c = (pitch)/(slope*2*pi)-(1/k4);
%
maxbeta = 1.0;
theta = 1.00;
beta = 0.85;
basedbeta = maxbeta/1000;
loading = 1.0;

while (loading == 1.0)
  k2 = 1/(beta*c);
  k3 = 1/(alpha*(1-beta)*c);
  %
  freedof = 2*n;
  fixeddof = 2;
  dof = 2*n+2;
  %
  Kff = zeros(freedof,freedof);
  Kfs = zeros(freedof,fixeddof);
  Kss = zeros(fixeddof,fixeddof);
```

```
    %
    [Kff] = freefreeK(k1,k2,k3,k4,alpha,freedof);
    [Kfs] = FreeFixedK(k1,k2,k3,k4,alpha,freedof,fixeddof);
    [Kss] = FixedFixedK(k1,k2,k3,k4,alpha,freedof,fixeddof);
    %
    % Set Free forces
    %
    Ff=zeros(freedof,1);
    %
    % Displace node
    %
    Us = [pitch*theta/(2*pi);0.0];

    [Uf]=freedisplacements(Kff,Kfs,Us);

    [Fm]=memberforces(Uf,Us,n,k1,k2,k3,k4,alpha);
    %
    % Check percent difference b/t experimental stiffness value and numerical value.
    %
    a = abs((Fm(n+1)-stiffness)/((Fm(n+1)+stiffness)/2));
    %
    % If the difference is less than 0.002 use that value for beta. If not do it again.
    % Beta will increase by 0.001.
    %
    if (d == 7/8.0)
      b = 0.0021;
    else
      b = 0.002;
    end
    %
    if (a < b)
      Kff;
      Uf;
      a;
      loading = -1.0;
      beta;
      ThreadLoadDist = Fm(1:n);
      BoltForce = Fm(n+1);

    else
      beta += basedbeta;
    end


  end
  %{
  theta = 3.11

  Us = [pitch*theta/(2*pi);0.0];

  [Uf]=freedisplacements(Kff,Kfs,Us);

  F1=[Fm]=memberforces(Uf,Us,n,k1,k2,k3,k4,alpha)


  %}
  ForceVector = [];
  Ufvector = [];



  theta = 0.125;
  basedtheta=0.125;


  while theta~=4.00


    Us = [pitch*theta/(2*pi);0.0];
```

```
136
137     [Uf]=freedisplacements(Kff,Kfs,Us);
138
139     F1=[Fm]=memberforces(Uf,Us,n,k1,k2,k3,k4,alpha);
140
141     ForceVector = [ForceVector; F1];
142     Ufvector = [Ufvector;Uf(2*n-1)];
143
144     theta +=basedtheta;
145
146   end
147
148   % Outputs to text file for easy plotting in excel
149   A = transpose(ForceVector(:,n+1));
150   B = transpose(Ufvector);
151
152   fileID = fopen('InitialPretension.txt','w');
153   fprintf(fileID,'%6.2f\r\n',A);
154   fclose(fileID);
155
156   fileID = fopen('UfDisplacement.txt','w');
157   fprintf(fileID,'%6.5f\r\n',B);
158   fclose(fileID);
159
160   fprintf('\r\n')
161   fprintf('Done')
162
163
```

```
function [Kff] = freefreeK(k1,k2,k3,k4,alpha,freedof);
%
% reads in the four values of element stiffness, and assembles Kff to
% correct size, based on freedof
%
Kff = zeros(freedof,freedof);
for i = 1:2:(freedof-3);
  Kff(i,i)=Kff(i,i)+k2+k1;
  Kff(i,i+1)=Kff(i,i+1)-k2;
  Kff(i+1,i)=Kff(i+1,i)-k2;
  Kff(i,i+2)=Kff(i,i+2)-k1;
  Kff(i+2,i)=Kff(i+2,i)-k1;
  Kff(i+1,i+1)=Kff(i+1,i+1)+k2;
  Kff(i+2,i+2)=Kff(i+2,i+2)+k1;
end
for j = 2:2:(freedof-2);
  Kff(j,j)=Kff(j,j)+k3;
  Kff(j+2,j+2)=Kff(j+2,j+2)+k3;
  Kff(j,j+2)=Kff(j,j+2)-k3;
  Kff(j+2,j)=Kff(j+2,j)-k3;
end
if freedof > 1
    n=freedof;
  Kff(n-1,n-1)=Kff(n-1,n-1)+k2+k4;
  Kff(n-1,n)=Kff(n-1,n)-k2;
  Kff(n,n-1)=Kff(n,n-1)-k2;
  Kff(n,n)=Kff(n,n)+k2;
end
Kff(n,n)=Kff(n,n)+alpha*k3;
Kff;
```

```
function [Kfs] = FreeFixedK(k1,k2,k3,k4,alpha,freedof,fixeddof);
%
% reads in the four values of element stiffness, and assembles Kfs to
% correct size, based on freedof and fixeddof
%
Kfs = zeros(freedof,fixeddof);
Kfs(freedof-1,1)= Kfs(freedof-1,1)-k4;
Kfs(freedof,2)= Kfs(freedof,2)-alpha*k3;
Kfs;
```

```
function [Uf]=freedisplacements(Kff,Kfs,Us)
% solves for free degree of freedom displacements
%

Kff;

Kffinverse=Kff^-1;
Uf = -1*Kfs*Us;
Uf=Kffinverse*Uf;

```

```
function [Kss] = FixedFixedK(k1,k2,k3,k4,alpha,freedof,fixeddof);
  %
  % reads in the four values of element stiffness, and assembles Kss to
  % correct size, based on fixeddof
  %
  Kss = zeros(fixeddof,fixeddof);
  Kss(1,1)=Kss(1,1)+k4;
  Kss(2,2)=Kss(2,2)+alpha*k3;


```

```
function [Fm]=memberforces(Uf,Us,n,k1,k2,k3,k4,alpha);
% takes displacement vector and determines member forces.
%
% n = number of threads engaged
%
% member #   description   dof1        dof2
%   1        1st thread    Us(1)       Uf(2n-1)
%   2        2nd thread    Uf(2n-2)    Uf(2n-3)
%   i        ith thread    Uf(2n+2-2i) Uf(2n+1-2i)
%   n        nth thread    Uf(1)       Uf(2)
%   n+1      bolt          Us(2)       Uf(2n-1)
Fm(n+1) = k4*(Us(1)-Uf(2*n-1));
for i = 1:n;
  Fm(i)=k2*(Uf(2*n+2-2*i)-Uf(2*n+1-2*i));
end
```

```
% ElasticBolt
%
% Elastic analyses of nut and bolt with n threads engaged.
%
%-------------------------------------------------------------
% Input Variables
%-------------------------------------------------------------
% n = number of threads that are engaged
% pitch = length of 1 full revolution of thread
% d = bolt diameter (inches)
% shank = length of shank (inches)
% lclamp = clamp length of assembly
%
%-------------------------------------------------------------
% Calculated Geometry Variables
%-------------------------------------------------------------
% athread = nominal area of threaded region
% ashank = area of shank region
%
%-------------------------------------------------------------
% Stiffness Variables
%-------------------------------------------------------------
% k1 = stiffness of one thread worth of bolt
% k2 = stiffness of interaction between one ring of threads
% k3 = stiffness of one thread worth of nut
% k4 = stiffness of clamped length of bolt
% [Kff] = stiffness of free dof
% [Kss] = stiffness of fixed dof
% [Kfs] = stiffness on free-fixed interaction
%
%-------------------------------------------------------------
% Displacement Variables
%-------------------------------------------------------------
% [Uf] = displacements of free nodes
% [Us] = displacements of specified nodes
%
%-------------------------------------------------------------
% Load Variables
%-------------------------------------------------------------
% [Pf] = external loads on free nodes
% [Ps] = resultant loads on specified nodes
%
%-------------------------------------------------------------
% Matrix Related Variables
%-------------------------------------------------------------
% dof = number of degrees of freedom (2*n+1)
% freedof = number of free degrees of freedom (2n-1)
% fixeddof = number of fixed degrees of freedom (2)
%
%-------------------------------------------------------------
% Other Variables
%-------------------------------------------------------------
% theta = twist of the nut past snug (radians)
%
%-------------------------------------------------------------

disp(' ')
%
prompt = 'Press 1 for 7/8" diameter and 2 for 3/4" diameter: ';
%
result = input(prompt);

if (result == 1)
  n = 7;
  d = 7/8.0;
  pitch = 0.11;
  slope = 7.966;
  lclamp = 1.95;
  shank = 1.88;
```

```
    beta = 0.933
    fy=-10.0;

  else
    n = 6;
    d = 3/4.0 ;
    pitch = 0.10;
    slope = 7.963775;
    lclamp = 2.07;
    shank = 2.00;
    beta = 0.872
    fy=-11.0;
  end

  tolerance= 0.001;
  E = 29000;
  pi= 3.14159265359;
  %
  factor = 0.95;
  alpha = 2.0;
  ashank = pi*d^2/4.0;
  athread = 0.785*(d-0.9743*pitch)^2;
  anut = pi*((d+0.25)^2-d^2)/4.0;
  %
  freedof = 2*n;
  fixeddof = 2;
  dof = 2*n+2;
  %
  k1 = athread*E/pitch
  k4 = 1/(1/(alpha*k1)+shank/(ashank*E)+(lclamp-shank+d/3)/(athread*E))
  c = (pitch)/(slope*2*pi)-(1/k4);
  %k2 = 1/(beta*c)
  % = 1/(alpha*(1-beta)*c)



  % k2 = 635.62
  % k3 = 2165.1
  k2 = 520.77
  k3 = 3626.0
  %
  Kff = zeros(freedof,freedof);
  Kfs = zeros(freedof,fixeddof);
  Kss = zeros(fixeddof,fixeddof);
  Us=[0.0;0.0];
  Fm=zeros(1,n+1);
  Uf=zeros(2*n,1);
  %
  [Kff]=freefreeK(k1,k2,k3,k4,alpha,freedof);
  [Kfs] = FreeFixedK(k1,k2,k3,k4,alpha,freedof,fixeddof);
  [Kss] = FixedFixedK(k1,k2,k3,k4,alpha,freedof,fixeddof);
  %
  % Set Free forces
  %
  Ff=zeros(freedof,1);
  %
  % Displace node
  %
  maxtheta = 4.000;
  loading = 1.0;
  basedtheta = maxtheta/14.5;
  theta = 0;
  Yieldedmember = 0;
  Yield = zeros(1,n);
  k = 0;

  % NEW NOTE 9/30/15

  %{ This loop is the only major difference from the elastic code. It just adjusts the
```

```
    stiffness
139 values for the yielded thread (the yield value was experimentally found. 10k for 7/8" & 11k
    for
140 3/4". The adjustment is based on a percent reduction of the original stiffness. The
    corresponding
141 subroutines are checkyield and EPmemberforces.
142 %}
143
144 while (loading==1)
145   if (theta+basedtheta>maxtheta)
146     dtheta = maxtheta-theta;
147   else
148     dtheta=basedtheta;
149   end
150   dUs = [pitch*dtheta/(2*pi);0.0];
151   [dUf]=freedisplacements(Kff,Kfs,dUs);
152   [dFm]=memberforces(dUf,dUs,n,k1,k2,k3,k4,alpha);
153   [fraction,Yieldedmember]=checkyield(Fm,dFm,Yield,fy,n);
154   [dFm]=EPmemberforces(dUf,dUs,n,k1,k2,k3,k4,alpha,Yield,fraction);
155   Yieldedmember;
156   if (Yieldedmember>0)
157     Yield(Yieldedmember)=Yield(Yieldedmember)+1;
158 %   change Kff here
159
    Kff(2*n-2*Yieldedmember+1,2*n-2*Yieldedmember+1)=Kff(2*n-2*Yieldedmember+1,2*n-2*Yieldedmembe
    r+1)-factor*k2;
160
    Kff(2*n-2*Yieldedmember+2,2*n-2*Yieldedmember+2)=Kff(2*n-2*Yieldedmember+2,2*n-2*Yieldedmembe
    r+2)-factor*k2;
161
    Kff(2*n-2*Yieldedmember+1,2*n-2*Yieldedmember+2)=Kff(2*n-2*Yieldedmember+1,2*n-2*Yieldedmembe
    r+2)+factor*k2;
162
    Kff(2*n-2*Yieldedmember+2,2*n-2*Yieldedmember+1)=Kff(2*n-2*Yieldedmember+2,2*n-2*Yieldedmembe
    r+1)+factor*k2;
163   end
164   Fm=Fm+fraction*dFm
165   Uf=Uf+fraction*dUf;
166   theta = theta+fraction*dtheta
167   %
168   fileID = fopen('output.txt','w');
169   fprintf(fileID,'%0.3f\r\n',Fm);
170   fclose(fileID);
171   %
172   if (theta>maxtheta-tolerance)
173     loading = -1.0
174   end
175   k = k+1
176   results(k,1) = theta;
177   results(k,2)=Fm(n+1);
178   results(k,3)=Yieldedmember;
179 end
180 %
181 %-------------------------------------------------------------
182 %-------------------------------------------------------------
183 %
184 %
185
186
187
188
189
190
```

```
function [Fm]=EPmemberforces(Uf,Us,n,k1,k2,k3,k4,alpha,Yield,fraction);
% takes displacement vector and determines member forces.
%
% n = number of threads engaged
%
% member #   description   dof1        dof2
%   1        1st thread    Us(1)       Uf(2n-1)
%   2        2nd thread    Uf(2n-2)    Uf(2n-3)
%   i        ith thread    Uf(2n+2-2i) Uf(2n+1-2i)
%   n        nth thread    Uf(1)       Uf(2)
%   n+1      bolt          Us(2)       Uf(2n-1)
Fm(n+1) = k4*(Us(1)-Uf(2*n-1));
for i = 1:n;
  if (Yield(i)==0)
    Fm(i)=k2*(Uf(2*n+2-2*i)-Uf(2*n+1-2*i));
  else
    Fm(i)=(1-fraction)*k2*(Uf(2*n+2-2*i)-Uf(2*n+1-2*i));
  end
end
```

```
function [Cdd] = slaveslaveC(c1,depdof);
%
% reads in the five values of element stiffness, and assembles Kfs to
% correct size, based on depdof
%
Cdd = zeros(depdof,depdof);
for i = 1:depdof;
  Cdd(i,i)=Cdd(i,i)+c1;
end
Cdd;
```

```
function [Cdf] = slavefreeC(c1,freedof,depdof);
%
% reads in the value of dampening constant, and assembles Cff to
% correct size, based on freedof and depdof
%
Cdf = zeros(depdof,freedof);

Cdf(1,1) = Cdf(1,1)-c1;


n=1;
m=1;
while n~=depdof && m~=freedof;
  n+=1;
  m+=2;
  Cdf(n,m) = Cdf(n,m)-c1;

end
```

```
function [Cfd] = freeslaveC(c1,freedof,depdof);
%
% reads in the five values of element stiffness, and assembles Kfs to
% correct size, based on depdof and freedof
%



Cfd = zeros(freedof,depdof);

Cfd(1,1) = Cfd(1,1)-c1;


n=1;
m=1;
while n~=freedof && m~=depdof
  n+=2;
  m+=1;
  Cfd(n,m) = Cfd(n,m)-c1;

end
```

```
function [Cff] = freefreeC(c1,freedof);
%
% reads in the value of dampening constant, and assembles Cff to
% correct size, based on freedof
%
Cff = zeros(freedof,freedof);

for i = 1:2:(freedof-3);
  Cff(i,i)=Cff(i,i)+c1;
end

if freedof > 1
    n=freedof;
  Cff(n-1,n-1)=Cff(n-1,n-1)+c1;
end
```

```
function [D1] = matrixD1(freedof,depdof);

D1 = zeros(depdof,freedof);

D1(1,1) = D1(1,1)+1;


n=1;
m=1;
while n~=depdof && m~=freedof;
  n+=1;
  m+=2;
  D1(n,m) = D1(n,m)+1;
end


```

```
function [Uf]=freedisplacements(Kff,Kfs,Kfd,Kdf,Us,D1,D2,s,c1,k1,k2,k5,Cfd,Cff,Cdd,Kdd)
% solves for free degree of freedom displacements in time dependent simulation
%



inverse=[Kff + (Kfd*D1) - (Cfd*((Cdd)^-1))*(Kdf+(Kdd*D1))]^-1;
Uf = ((((Cfd*((Cdd)^-1))*Kdd)-Kfd)*s)-(Kfs*Us);
Uf=inverse*Uf;


```

```
function [Kdd] = slaveslaveK(k1,k2,k3,k4,k5,alpha,depdof);
%
% reads in the five values of element stiffness, and assembles Kfs to
% correct size, based on depdof
%
Kdd = zeros(depdof,depdof);
for i = 1:depdof;
  Kdd(i,i)=Kdd(i,i)+k5+k2;
end
Kdd;
```

```
function [Kdf] = slavefreeK(k1,k2,k3,k4,k5,alpha,freedof,depdof);
%
% reads in the five values of element stiffness, and assembles Kfs to
% correct size, based on depdof and freedof
%
Kdf = zeros(depdof,freedof);

Kdf(1,1) = Kdf(1,1)-k5;
Kdf(1,2) = Kdf(1,2)-k2;

n=1;
m=1;
while n~=depdof && m~=freedof;
  n+=1;
  m+=2;
  Kdf(n,m) = Kdf(n,m)-k5;

end

i=1;
j=2;
while i~=depdof && j~=freedof;
  i+=1;
  j+=2;
  Kdf(i,j) = Kdf(i,j)-k2;

end

Kdf;
```

```
function [Kfd] = freeslaveK(k1,k2,k3,k4,k5,alpha,freedof,depdof);
%
% reads in the five values of element stiffness, and assembles Kfs to
% correct size, based on depdof and freedof
%
Kfd = zeros(freedof,depdof);

Kfd(1,1) = Kfd(1,1)-k5;
Kfd(2,1) = Kfd(2,1)-k2;

n=1;
m=1;
while n~=freedof && m~=depdof
  n+=2;
  m+=1;
  Kfd(n,m) = Kfd(n,m)-k5;

end

i=2;
j=1;
while i~=freedof && j~=depdof
  i+=2;
  j+=1;
  Kfd(i,j) = Kfd(i,j)-k2;

end

Kfd;
```

```
function [Kff] = freefreeK(k1,k2,k3,k4,k5,alpha,freedof);
%
% reads in the five values of element stiffness, and assembles Kff to
% correct size, based on freedof
%

Kff = zeros(freedof,freedof);
for i = 1:2:(freedof-3);
  Kff(i,i)=Kff(i,i)+k5+k1;
  Kff(i,i+2)=Kff(i,i+2)-k1;
  Kff(i+2,i)=Kff(i+2,i)-k1;
  Kff(i+1,i+1)=Kff(i+1,i+1)+k2;
  Kff(i+2,i+2)=Kff(i+2,i+2)+k1;
end
for j = 2:2:(freedof-2);
  Kff(j,j)=Kff(j,j)+k3;
  Kff(j+2,j+2)=Kff(j+2,j+2)+k3;
  Kff(j,j+2)=Kff(j,j+2)-k3;
  Kff(j+2,j)=Kff(j+2,j)-k3;
end
if freedof > 1
    n=freedof;
  Kff(n-1,n-1)=Kff(n-1,n-1)+k5+k4;
  Kff(n,n)=Kff(n,n)+k2;
end
Kff(n,n)=Kff(n,n)+alpha*k3;
```

```
function [Kfs] = FreeFixedK(k1,k2,k3,k4,k5,alpha,freedof,fixeddof);
%
% reads in the four values of element stiffness, and assembles Kfs to
% correct size, based on freedof and fixeddof
%
Kfs = zeros(freedof,fixeddof);
Kfs(freedof-1,1)= Kfs(freedof-1,1)-k4;
Kfs(freedof,2)= Kfs(freedof,2)-alpha*k3;
Kfs;
```

```
function [Kss] = FixedFixedK(k1,k2,k3,k4,k5,alpha,freedof,fixeddof);
  %
  % reads in the four values of element stiffness, and assembles Kss to
  % correct size, based on fixeddof
  %
  Kss = zeros(fixeddof,fixeddof);
  Kss(1,1)=Kss(1,1)+k4;
  Kss(2,2)=Kss(2,2)+alpha*k3;


```

```
function [Fm]=memberforces(Uf,Us,n,k1,k2,k3,k4,s,alpha);
% takes displacement vector and determines member forces.
%
% n = number of threads engaged
%
% member #   description   dof1        dof2
%   1        1st thread    Us(1)       Uf(2n-1)
%   2        2nd thread    Uf(2n-2)    Uf(2n-3)
%   i        ith thread    Uf(2n+2-2i) Uf(2n+1-2i)
%   n        nth thread    Uf(1)       Uf(2)
%   n+1      bolt          Us(2)       Uf(2n-1)

for i = 1:n;
  Fm(i)=k2*(Uf(2*n+2-2*i)-Uf(2*n+1-2*i)-(flipud(s(i))));
end


%Fm(n+1) = k4*(Us(1)-Uf(2*n-1)+(s(n)));
Fm(n+1) = -1*sum(Fm(Fm<0));
```

```
function [Th]=threshold(k1,k2,k3,k4,Fthres,n,Kff2,Kfs,pitch,alpha)


A = -1*Kfs(2*n-1,1);
X = [Kff2]^-1;

%Find location of free fixed node displacement for threshold force
B=X(2*n-1,2*n-1);

G = zeros(2,1);
G(1,1) = (Fthres/k4);

F = -1*([A]*[B]*[G])/(([A]*[B])-1);
H = F(1,1);

Us1=zeros(2,1);
Us1(1,1)=(Fthres/k4) + H;

Us1;

[Uf2]=freedisplacements2(Kff2,Kfs,Us1);
[Fm2]=memberforces2(Uf2,Us1,n,k1,k2,k3,k4,alpha);


Th = flipud(transpose(Fm2(1:1:n)))*-1;



%Fm(n+1) = k4*(Us(1)-Uf(2*n-1)+(s(n)))
```

```
1
2   % Code simulating linear-elastic relaxation behavior
3
4   disp(' ')
5   %
6   prompt = 'Press 1 for 7/8" diameter and 2 for 3/4" diameter: ';
7   %
8   result = input(prompt);
9
10  % Inputs for 7/8" bolt
11  if (result == 1)
12    n = 7;
13    d = 7/8.0;
14    pitch = 0.11;
15    slope = 7.966;
16    lclamp = 1.96;
17    shank = 1.88;
18    beta = 0.933;
19    Fthres = 27.469;
20
21  % Inputs for 3/4" bolt
22  else
23    n = 6;
24    d = 3/4.0 ;
25    pitch = 0.10;
26    slope = 7.963775;
27    lclamp = 2.07;
28    shank = 2.00;
29    beta = 0.872;
30    Fthres = 20.604;
31  end
32
33
34  % Material properties, constants, and bolt dimensions
35  E = 29000;
36  pi= 3.14159265359;
37  alpha = 2.00;
38  ashank = pi*d^2/4.0;
39  athread = 0.785*(d-0.9743*pitch)^2;
40  anut = pi*((d+0.25)^2-d^2)/4.0;
41
42  %
43
44  % bolt stiffness, nut stiffness, POC stiffness
45  k1 = athread*E/pitch;
46  k4 = 1/(1/(alpha*k1)+shank/(ashank*E)+(lclamp-shank+d/3)/(athread*E));
47  c = (pitch)/(slope*2*pi)-(1/k4);
48  k2 = 1/(beta*c);
49  k3 = 1/(alpha*(1-beta)*c);
50  %
51  % Resistance stiffness to relaxation (k). dampening coefficient (c)
52  k5=714;
53  c1=60000;
54  % The units for c1 are kip-days per inch
55
56  % Define DOF (free, fixed, slaved)
57  freedof = 2*n;
58  fixeddof = 2;
59  dof = 3*n+2;
60  depdof = dof - freedof -fixeddof;
61  %
62  %
63  % Sets all matrix partitions as zero matrices to then assign values
64  %
65  Kff = zeros(freedof,freedof);
66  Kff2 = zeros(freedof,freedof);
67  Kfs = zeros(freedof,fixeddof);
68  Kss = zeros(fixeddof,fixeddof);
69  %
```

```
%
Kfd = zeros(freedof,depdof);
Kdf = zeros(depdof,freedof);
Kdd = zeros(depdof,depdof);
%
Cff = zeros(freedof,freedof);
Cfd = zeros(freedof,depdof);
Cdd = zeros(depdof,depdof);
%
%
%Location matrices (used to call out position of master nodes (Uf)
D1 = zeros(depdof,freedof);
D2 = zeros(freedof,depdof);
%
[Kff] = freefreeK(k1,k2,k3,k4,k5,alpha,freedof);
[Kff2] = freefreeK2(k1,k2,k3,k4,alpha,freedof);
[Kfs] = FreeFixedK(k1,k2,k3,k4,k5,alpha,freedof,fixeddof);
[Kss] = FixedFixedK(k1,k2,k3,k4,k5,alpha,freedof,fixeddof);
%
[Kfd] = freeslaveK(k1,k2,k3,k4,k5,alpha,freedof,depdof);
[Kdf] = slavefreeK(k1,k2,k3,k4,k5,alpha,freedof,depdof);
[Kdd] = slaveslaveK(k1,k2,k3,k4,k5,alpha,depdof);
%
[Cff] = freefreeC(c1,freedof);
[Cfd] = freeslaveC(c1,freedof,depdof);
[Cdd] = slaveslaveC(c1,depdof);
%
[D1] = matrixD1(freedof,depdof);
[D2] = matrixD2(freedof,depdof);


%
%
%
s = zeros(depdof,1);
s;
% Sets rotation angle (theta) and the resulting displacement (Us)
theta=2.87506064316966;


Us = [pitch*theta/(2*pi);0.0];
%
%
%[sdot] = dashpotvelocity(Kdf,Uf,s,Kdd,Cdd,D1);



% Outputs to text file for easy plotting in excel
ForceVector = [];
svector = [];

%[Uf]=freedisplacements(Kff,Kfs,Kfd,Kdf,Us,D1,D2,s,c1,k1,k2,k5,Cfd,Cff,Cdd,Kdd);


[Uf]=freedisplacements(Kff,Kfs,Kfd,Kdf,Us,D1,D2,s,c1,k1,k2,k5,Cfd,Cff,Cdd,Kdd);
F2 = [Fm]= memberforces(Uf,Us,n,k1,k2,k3,k4,s,alpha);


%Fph = [Fm]= memberforces(Uf,Us,n,k1,k2,k3,k4,s,alpha);

%Fpreten = -1*flipud(transpose(Fph(Fph<0)));


% Loops time steps to simulate relaxation
ds = zeros(depdof,1);
t=0;
while t~=500

  [Uf]=freedisplacements(Kff,Kfs,Kfd,Kdf,Us,D1,D2,s,c1,k1,k2,k5,Cfd,Cff,Cdd,Kdd);
```

```
    F1 = [Fm]= memberforces(Uf,Us,n,k1,k2,k3,k4,s,alpha);

    [Th]=threshold(k1,k2,k3,k4,Fthres,n,Kff2,Kfs,pitch,alpha);

    Fvel = (Kdf*Uf)+(Kdd*((D1*Uf)+ s));

    %if Fvel - Th < 0

     %   t = 500;

    %else



      if t < 1
        pct = F1(n+1);
      else
        pct;
      end

      force = F2(n+1);


      svel = (-1*((Cdd)^-1)*(Fvel-(Th)));

      sdot = 1*svel;

      dt = 1;
      ds = dt*sdot;

      s += ds;

      s=flipud(s);
      t+=1;

   % end


    ForceVector = [ForceVector; F1];
    svector = [svector;s(depdof)];


    pct = ForceVector(t,n+1);


  end



  % Outputs to text file for easy plotting in excel
  A = transpose(ForceVector(:,depdof+1));
  B = transpose(svector);

  fileID = fopen('BoltForce.txt','w');
  fprintf(fileID,'%6.2f\r\n',A);
  fclose(fileID);

  fileID = fopen('BoltDis.txt','w');
  fprintf(fileID,'%6.5f\r\n',B);
  fclose(fileID);

  fprintf('\r\n')


  pctloss = (1-((A(:,end))/(A(:,1))))*100;

  if pctloss > 0;

    X = ['The losses are ',num2str(pctloss),'%.'];
```

```
208
209   else
210
211   X = ['The losses are 0%.'];
212
213   end
214
215   disp(X)
216   disp(' ')
217
218   fprintf('Done')
```